Monthly Notices
of the
ROYAL ASTRONOMICAL SOCIETY

Mon. Not. R. Astron. Soc. **415,** 1549–1568 (2011) doi:10.1111/j.1365-2966.2011.18806.x

AGN feedback in galaxy groups: the delicate touch of self-regulated outflows

M. Gaspari,[1⋆] F. Brighenti,[1] A. D'Ercole[2] and C. Melioli[1]

[1]*Astronomy Department, University of Bologna, Via Ranzani 1, 40127 Bologna, Italy*
[2]*INAF-OABO, Via Ranzani 1, 40127 Bologna, Italy*

Accepted 2011 March 25. Received 2011 March 25; in original form 2011 February 8

ABSTRACT

Active galactic nucleus (AGN) heating, through massive subrelativistic outflows, might be the key to solve the long-lasting 'cooling flow problem' in cosmological systems. In a previous paper, we showed that cold accretion feedback and, to a lesser degree, Bondi self-regulated models are in fact able to quench cooling rates for several Gyr, at the same time preserving the main cool-core features, like observed density and temperature profiles. Is it true also for lighter systems, such as galaxy groups? The answer is globally yes, although with remarkable differences. Adopting a modified version of the adaptive mesh refinement code FLASH 3.2, we found that successful 3D simulations with cold and Bondi models are almost convergent in the galaxy group environment, with mechanical efficiencies in the range 5×10^{-4}–10^{-3} and 5×10^{-2}–10^{-1}, respectively. The evolutionary storyline of galaxy groups is dominated by a quasi-continuous gentle injection with sub-Eddington outflows (with the mechanical power $P \sim 10^{44}$ erg s^{-1}, $v \sim 10^4$ km s^{-1}). The cold and hybrid accretion models present, in addition, very short quiescence periods, followed by moderate outbursts (10 times the previous phase), which generate a series of 10–20 kpc size cavities with high density contrast, temperatures similar to the ambient medium and cold rims. After shock heating, a phase of turbulence promotes gas mixing and diffusion of metals, which peak along the jet-axis (up to 40 kpc) during active phases. At this stage, the tunnel, produced by the enduring outflow (hard to detect in the mock X-ray surface brightness maps), is easily fragmented, producing tiny buoyant bubbles, typically a few kpc in size. In contrast to galaxy clusters, the AGN self-regulated feedback has to be persistent, with a 'delicate touch', rather than rare and explosive strokes. This evolutionary difference dictates that galaxy groups are not scaled-down versions of clusters: AGN heating might operate in different regimes, contributing to the self-similarity breaking observed.

Key words: hydrodynamics – galaxies: active – galaxies: groups: general – intergalactic medium – galaxies: jets – x-rays: galaxies.

1 INTRODUCTION

Remarkably, most of the galaxies in the Universe reside in small groups (up to 70 per cent in the nearby zone; Geller & Hucra 1983; Mulchaey 2000). Nevertheless, relatively little attention has been devoted to groups with respect to their 'big brothers', galaxy clusters. Groups, with typical masses around 10^{13} M$_\odot$, are thus a key class of objects, containing a significant fraction of the overall universal baryon budget and being a nursery for massive (early-type) galaxies.

Galaxy groups are X-ray sources, with diffuse extended (50–500 kpc) emission similar to that of rich clusters, but with lower luminosities, ranging from 10^{41} erg s^{-1} up to several times 10^{43} erg s^{-1}, with temperatures around ∼0.3–2 keV (Mulchaey 2000).

It is known that clusters and groups do not follow the global scaling relations predicted by self-similar models (e.g. Kaiser 1986; Evrard & Henry 1991; Osmond & Ponman 2004; Vikhlinin et al. 2006). Groups are not perfect scaled-down versions of clusters. If groups are sampled at sufficiently large radii, some X-ray scaling relations (e.g. luminosity–temperature, mass–temperature) seem similar to those followed by massive clusters (Osmond & Ponman 2004; Sun et al. 2009), with the scatter increasing for $T \lesssim 1$ keV. However, systematic differences between groups and clusters exist, with the former having clearly lower gas (and baryon) fractions and flatter entropy profiles (Finoguenov et al. 2005; Voit 2005; Sun et al. 2009). Moreover, groups have velocity dispersions of several hundreds of

⋆E-mail: massimo.gaspari4@unibo.it

km s^{-1}, comparable to the internal velocity dispersion of individual galaxies. For this reason, some processes are more (merging) or less (ram-pressure stripping, galaxy harassment) relevant than in clusters.

The discrepancies between the observed scaling relations and the predictions of self-similar models, and especially the systematic differences between groups and clusters quoted above, can be explained by the presence of non-gravitational heating, acting during or after the gravitational collapse. In lower mass systems, the same amount of energy per unit mass has a stronger effect. This is a key point for the mechanical active galactic nucleus (AGN) feedback problem investigated here and in our previous work (Gaspari et al. 2011, hereinafter G11).

As in clusters and elliptical galaxies, many galaxy groups display the typical signatures of cooling flows (CFs)[1] (a most notable example being NGC 5044). At the centre, where the radiative cooling time is the shortest ($\sim 10^7$ yr), the temperature of the intragroup medium (IGM) drops by nearly 50 per cent. Moreover, the X-ray surface brightness is sharply peaked, with the maximum coincident with a massive elliptical galaxy.

A large sample of X-ray groups are presented in Sun et al. (2009). Gathering 43 objects with *Chandra* data, they confirmed the existence of a 'universal' temperature profile (De Grandi & Molendi 2002; Voit 2005; Leccardi & Molendi 2008). The group profiles are slightly steeper than those of clusters for $r \geq 0.15 r_{500}$. In the inner cool core, the scatter is significant: the majority present positive gradients, while few are approaching a flat temperature profile (a possible signature of a heating cycle). Sun et al. produced also the entropy profiles, which retain the thermal history of the gas. They again confirmed previous important works (Ponman, Cannon & Navarro 1999; Finoguenov et al. 2002; Ponman, Sanderson & Finoguenov 2003), suggesting deviations in the entropy from the self-similar relation ($K \propto T$), showing a clear flat core, and an excess relative to massive clusters.

One of the most striking riddles of galaxy group astrophysics concerns the so-called 'cooling flow problem'. This paper attempts to solve it, finding plausible consistent models, as has been done for galaxy clusters in G11. The classical CF model (Fabian 1994 for a review) predicts that as the gas radiates, its entropy decreases and thus gets compressed by the surrounding gas, causing it to subsonically flow inwards. The estimated (isobaric) cooling rate is given by

$$\dot{M} \simeq \frac{2}{5} \frac{\mu m_{\rm p}}{k_{\rm B} T} L_{\rm X}, \quad (1)$$

where $L_{\rm X}$ is the X-ray luminosity, μ is the mean molecular weight, $k_{\rm B}$ is the Boltzmann constant and $m_{\rm p}$ is the proton mass. For typical luminosities of groups ($\approx 10^{43}$ erg s^{-1}), the relation implies cooling rates of several tens of $M_\odot$ yr^{-1}. Such high predicted $\dot{M}$ have been in contrast for years to the estimates of star formation rates and cold gas masses (at least an order of magnitude lower), but the definitive observational evidence against the traditional CF model has been the spectral analysis of XMM-RGS spectra (e.g. Peterson et al. 2001, 2003; Tamura et al. 2003; Peterson & Fabian 2006).

In the last decade, the new-generation *XMM–Newton* and *Chandra* telescopes have radically changed the panorama of the evolution of hot gas in groups and clusters. The *ROSAT*-HRI and, especially, *Chandra* high-resolution X-ray images show clear evidence of the AGN–gas interaction from giant elliptical galaxies (gEs) to clusters (Böhringer et al. 1993; Blanton et al. 2001; Finoguenov & Jones 2001; Jones et al. 2002; McNamara & Nulsen 2007, and references therein). Evidence of such activity has also been identified in several groups (Allen et al. 2006; Morita et al. 2006; Jetha et al. 2008; Gastaldello et al. 2009; Giacintucci et al. 2011). The fairly common presence of X-ray cavities, often coincident with lobes of radio emission connected to the core of the central galaxy by a radio jet, indicates that AGNs inject energy in the IGM in kinetic form (outflows) and as relativistic particles.

Moreover, from dozens of gEs (Nulsen et al. 2007) to rich clusters (Rafferty et al. 2006; Rafferty, McNamara & Nulsen 2008), there is a continuous scaling relation between the AGN power, associated with the cavity formation, and the core X-ray luminosity. This trend is more evident in low-mass systems. Although this connection is likely to be a necessary but not sufficient requirement for a successful heating scenario, it strongly suggests that the dominant heating process manifests itself generating bubbles in the intergalactic medium, through some kind of 'directional' energy input, such as jets or collimated outflows (rather than spherically symmetric forms).

AGN outflows seem to be a very promising mechanism to simultaneously explain the quenching of CFs (and star formation), the deviation of scaling relations from self-similar laws and the presence of X-ray cavities and weak shocks in the intergalactic (interstellar) medium. As anticipated before, the impact of this type of heating is much more evident in less bounded systems, such as groups. We can therefore speculate that gentler outflows are more appropriate to regulate the thermodynamic evolution of the IGM, while strong bursts should easily deform the main properties.

Regarding clusters, we can account for several variegated computations (e.g. Omma et al. 2004; Ruszkowski, Brüggen & Begelman 2004; Brüggen, Ruszkowski & Hallman 2005; Brighenti & Mathews 2006; Sternberg, Pizzolato & Soker 2007; Gaspari et al. 2009; G11, among others), but little work has been done to explore the role of AGN heating on the IGM, especially from a theoretical and numerical point of view. Brighenti & Mathews (2003) studied thermal heating (plus conduction) in 2D simulations, showing that this type of feedback, while very efficient in stopping the cooling process, often generates negative temperature gradients, with the total erasure of galactic CFs commonly observed in gEs (Sun et al. 2005, 2007). Carrying out cosmological simulations (Puchwein, Sijacki & Springel 2008; McCarthy et al. 2010) does not permit, nowadays, a detailed analysis of the feedback dynamics in the inner cool core, mainly because of the lack of resolution, and are thus more suited to study global sample-averaged properties. Further, none of the above mentioned works has investigated a purely mechanical feedback.

In this paper, we will therefore describe, for the first time, 3D self-regulated hydrodynamical simulations of AGN outflows in an exemplary galaxy group, lasting at least 7 Gyr. The positive results of similar simulations for rich galaxy clusters (G11) are a strong motivation for a detailed analysis of this (mechanical) feedback mechanism in lower mass systems.

As in G11, we assume that AGN outflows are the key element in solving the cooling flow problem. The physical foundation is that the relativistic jet, produced by the active nucleus, entrains ambient gas, strongly decelerating within a scalelength of just a few kpc. Such subrelativistic AGN outflows have been observed in several cD galaxies in every band, thanks to blueshifted absorption lines: optical (Nesvadba et al. 2008, 2011), ultraviolet and X-ray (see Crenshaw, Kraemer & George 2003, for a review), and 21 cm (Morganti, Tadhunter & Oosterloo 2005; Morganti et al.

[1] Interestingly, the analogues of non-cool-core clusters on the group scale have been rarely detected (Johnson et al. 2011).

2007; see also the references in G11). They usually occur at a distance of about a kpc with velocities ranging from several 1000 to several 10000 km s^{-1} (see also Tombesi et al. 2010). The geometry of the bipolar outflows is still unclear, with usually narrow opening angles and possibly some kind of precession.

The timing of the feedback is also an important issue. From observations and from a 'thermostat' assumption, the duty cycle has to be similar to the cooling time, around 10^7 yr. We will simplify the feedback self-regulation, testing hot (Bondi) or cold accretion models with different mechanical efficiencies. Fully 3D simulations are required to compute the chaotic and turbulent flow, with associated instabilities.

In summary, this work will focus on a set of heated CF models with a variety of AGN feedback mechanisms, aimed to answer the following key question: *are AGN outflows able to prevent the IGM from cooling and at the same time preserve the observed cool-core appearance for many Gyr?*

2 THE COMPUTATIONAL PROCEDURE

In order to study the behaviour of AGN outflows in galaxy groups, we carried out several simulations with a substantially modified version of FLASH 3.2 (Fryxell et al. 2000), a popular 3D adaptive mesh refinement (AMR) code. FLASH uses the Message-Passing Interface library to achieve portability and efficient scalability on a variety of different parallel high-performance computing systems. The simulations were usually run on 128 processors of IBM P575 Power 6 (SP6) at the CINECA supercomputing centre.

We tested different numerical schemes to solve the hydrodynamic Euler equations. As in G11, we widely used the Piecewise-Parabolic Method (PPM) solver (Colella & Woodward 1984), particularly appropriate to describe shock fronts. It uses directional splitting to advect quantities (Strang 1968). This makes the instantaneous injection of the outflow not trivial, since we must manage two equal time-steps with a sweep *x*–*y*–*z* and then *z*–*y*–*x*. Thus, we decided to also adopt other unsplit methods (single time-step evolution). We tested Roe and Lax-Friedrichs, with different slope limiters (van Leer, minmod, etc.). They work pretty well for smooth flows, but not for a powerful jet ignition, producing unstable results also with low Courant–Friedrichs–Lewy (CFL) numbers (<0.1). On the contrary, the HLLC solver (Toro 1999) is very stable also for higher CFL numbers (∼0.5), with a good description of shocks and contact discontinuities. In the end, results with both methods are comparable, with the PPM being more accurate (third order), while the HLLC is faster and more manageable. In many cases, we preferred accuracy over speed.

The innovations implemented in FLASH reside, mainly, in several source and sink terms added to the usual hydro-equations. In conservative form

$$\frac{\partial \rho}{\partial t} + \nabla \cdot (\rho \boldsymbol{v}) = \alpha \rho_* - q \frac{\rho}{t_{\rm cool}} + S_{1,\rm jet}\,, \tag{2}$$

$$\frac{\partial \rho \boldsymbol{v}}{\partial t} + \nabla \cdot (\rho \boldsymbol{v} \otimes \boldsymbol{v}) + \nabla P = \rho \boldsymbol{g}_{\rm DM} + S_{2,\rm jet}\,, \tag{3}$$

$$\frac{\partial \rho \varepsilon}{\partial t} + \nabla \cdot [(\rho \varepsilon + P)\,\boldsymbol{v}] = \rho \boldsymbol{v} \cdot \boldsymbol{g}_{\rm DM} + \alpha \rho_* \left(\varepsilon_0 + \frac{\boldsymbol{v}^2}{2}\right) - n_{\rm e} n_{\rm i} \Lambda(T, Z) + S_{3,\rm jet}, \tag{4}$$

$$P = (\gamma - 1)\,\rho \left(\varepsilon - \frac{\boldsymbol{v}^2}{2}\right), \tag{5}$$

where ρ is the gas density, $\boldsymbol{v}$ is the velocity, ε the specific total energy (internal and kinetic), P is the pressure, $\boldsymbol{g}_{\rm DM}$ is the gravitational acceleration (due to the dark matter halo plus the central elliptical, see below) and $\gamma = 5/3$ is the adiabatic index. The temperature is computed from P and ρ using equation (5), with an atomic weight $\mu \simeq 0.62$, appropriate for a totally ionized plasma with 25 per cent He in mass.

In G11, we describe in depth all the source and sink terms (right-hand side of the first three equations). Here we give a summary.

Radiative cooling is modelled according to the Sutherland & Dopita (1993) cooling function $\Lambda(T, Z)$ for a fully ionized plasma ($n_{\rm e}$ and $n_{\rm i}$ are the number density of electrons and ions). For typical groups, the central metallicity Z is about solar (e.g. Rasmussen & Ponman 2009), with a negative gradient at larger radii. For simplicity, we set the abundance equal to 1 $Z_\odot$.

Supernovae Ia (SNeIa) and stellar winds (SWs) in the central elliptical galaxy are implemented following Brighenti & Mathews (2002), with the stellar mass-loss rate $\alpha(t)$ dominated by SWs $\propto t^{-1.3}$.

The key prescription for treating the cold gas is the dropout term (equation 2), proportional to $q = 2\exp[-(T/5 \times 10^5)^2]$. It removes the gas below $T = 10^4$–10^5 K, whose physical evolution cannot be properly followed by our code.[2] Because it has been proved that the total mass of cooled gas is insensitive to the presence of the dropout term or its functional form (see Brighenti & Mathews 2000), we can still calculate the gas cooling rate accurately.

Outflow source terms $S_{1,2,3,\rm jet}$ will be explained for every type of feedback in Section 2.2. Injection will be done with two different methods: directly into the domain (without a mass inflow) or through a boundary condition at $z = 0$ ($S_1 > 0$).

We calculate the flow evolution for 7 Gyr. Local cosmological systems have very different formation times and are subject to relatively frequent mergers (Cohn & White 2005). We conservatively decided to run our simulations for such a long time to take into account the systems which do not undergo major mergers since $z \sim 0.7$. Moreover, cool cores in massive objects may survive major mergers (e.g. Burns et al. 2008), implying that the central AGN feedback is continuously needed.

Note that several feedback schemes could delay excessive gas cooling for only 1 Gyr before failing (see G11). Thus, we stress that a few hundreds of Myr evolution is not sufficient to make predictions on the heating versus cooling regulation and might lead to misleading extrapolations.

2.1 The group model and initial conditions

We choose NGC 5044 as the template for a typical X-ray bright group of galaxies: all the results we present should be relevant for any object in this category. NGC 5044 was one of the first cool-core groups observed, due to its high X-ray brightness, with low redshift 0.009 (see Buote et al. 2003; Gastaldello et al. 2009; David et al. 2009, for recent *Chandra* and *XMM* data). The estimated X-ray bolometric (0.1–100 keV) luminosity is around 2×10^{43} erg s^{-1}, with a virial mass of $\sim 4 \times 10^{13}$ $M_\odot$. The large-scale morphology is very smooth and nearly spherical, despite a little disturbance in the form of a south-eastern cold front. On the contrary, the core (∼10 kpc) has been strongly perturbed by recent outbursts from the central AGN. The group presents many small radio-quiet cavities

[2] Tests without the dropout show the artificial assembly of cold clumps near the centre.

with a nearly isotropic distribution and moderate mechanical power ($\sim 10^{42}$ erg s^{-1}). The two biggest cavities at larger radii (10–20 kpc) are instead filled with radio emission at 235 MHz (David et al. 2009) and the associated mechanical power seems to be able to balance radiative losses. The NGC 5044 X-ray image also shows several cold filaments coincident with Hα and dust emission, indicating a physical connection between the various gas phases (Gastaldello et al. 2009). The GMRT observation (610 MHz) reveals the presence of extended radio emission with a torus-like morphology, threaded by the largest filament (probably cold material being uplifted from the centre).

The cooling time of the hot gas within the central 2 kpc is just $\sim 4 \times 10^7$ yr. In the absence of feedback, a pure CF model predicts tens of $M_\odot$ yr^{-1} (see equation 1), while observations suggest that the cooling rate is at least an order of magnitude lower, less than a few $M_\odot$ yr^{-1} (David et al. 2009). This is the key requirement for our computed models.

This galaxy group consists of a luminous gE (NGC 5044) surrounded by a cluster of $\sim$150 low-luminosity dwarf galaxies, mostly of early type. Thus, we choose to model the elliptical galaxy with a de Vaucouleurs profile (Mellier & Mathez 1987) with the total stellar mass $M_* \sim 3.4 \times 10^{11}\, M_\odot$ and effective radius $r_e \sim 10$ kpc (Buote, Brighenti & Mathews 2004).

We start our calculations with the hot gas in spherical hydrostatic equilibrium in the potential well generated by the total system mass. We use the observed $T(r)$ and $n(r)$ (Buote et al. 2003, 2004, see the dotted lines in Fig. 1) to calculate the total gravitational potential under the assumption of hydrostatic equilibrium. At the virial radius, the gas fraction is $\sim$0.11, a reasonable value for X-ray bright groups (Mathews et al. 2005).

The computational rectangular 3D box in all of our models extends slightly beyond the group virial radius, R_{104}. We simulate the $z \geq 0$ half-space with a symmetric boundary condition at $z = 0$, while elsewhere we set prolonged initial conditions with only outflows allowed. Despite the AMR capability of FLASH, we decided to use a number of concentric fixed grids in Cartesian coordinates. This ensures a proper resolution of the waves and cavities generated in the cluster core by the AGN outflows. We use a set of 10 grid levels (basic blocks of $8 \times 8 \times 4$ points), with the zone linear size doubling among adjacent levels. The finest, inner grid has a resolution of 488 pc and covers a spherical region of $\sim$20 kpc in radius. In general, grids of every level extend radially for about 40 cells. This simple method is the best way found to cover large spatial scales (hundreds of pc up to Mpc) and at the same time integrating the system for several Gyr, using moderate computing resources.

2.2 Outflow generation

We adopt a purely mechanical AGN feedback in the form of non-relativistic, collimated outflows. The implementation is similar to the galaxy cluster outflows of G11.

In considering massive slow outflows, we are implicitly assuming that the relativistic jet entrains some ICM mass ($M_{\rm act}$) or, in a similar way, that radio jets are highly relativistic on pc scale, but rapidly decrease to subrelativistic velocities within few kpc from the black hole (BH) (Giovannini 2004).

As in G11 we show results only for models with cylindrical jets, with the velocity parallel to the z-axis. We have calculated few simulations with conical (or precessing) outflows and verified that they have a similar impact on the global properties of the flow. In fact, the pressure of the surrounding gas collimates the outflows within few tens of kpc.

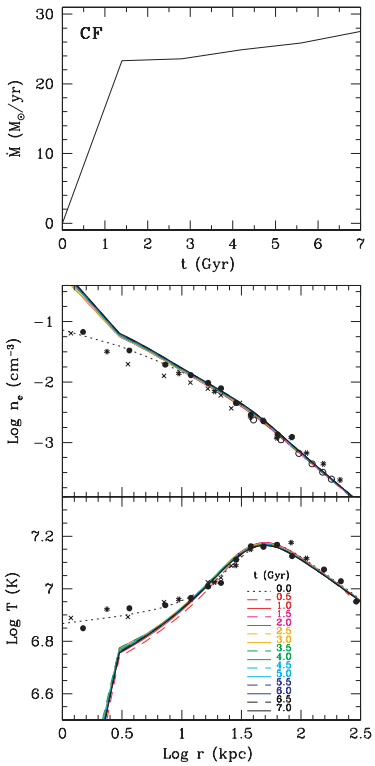

Figure 1. Evolution of a CF model (no AGN feedback). Top panel: gas cooling rate versus time. Middle and bottom panels: temporal evolution of the gas (electron) number density and mass-weighted temperature profiles, respectively. The profiles are displayed at 15 different times, as indicated in the lowermost panel. *Chandra* and *XMM–Newton* observational data of NGC 5044 are represented by the star and cross points (Buote et al. 2004), and filled circles (Buote et al. 2003); the open circles indicate *ROSAT* data (David et al. 1994).

In this paper, we will focus mainly on the two most successful models adopted for clusters in G11: cold and Bondi feedback.

In the cold feedback,[3] an outflow is activated only when gas cools to very low temperature within a spherical region $r < 3$ kpc and drops out from the flow. If $\Delta M_{\rm cool}$ is the mass cooled in the aforementioned region during a single time-step, the injected kinetic energy (in the following time-step) is given by

$$\Delta E_{\rm jet} = \epsilon\, \Delta M_{\rm cool}\, c^2. \tag{6}$$

This energy is given to the hot gas located in a small region at the centre of the grid (the 'active jet region'), whose size is always[4] 2×4 cells ($\sim$1 kpc wide, 2 kpc high), containing a hot gas mass $M_{\rm act}$:

$$\frac{1}{2} M_{\rm act} v_{\rm jet}^2 = \Delta E_{\rm jet}. \tag{7}$$

We will see that the frequency and strength of the feedback events strongly depend on the mechanical efficiency ϵ, which has typical values 10^{-4}–10^{-3} (see Table 1), almost an order lower than galaxy clusters.

[3] See also Soker (2006) for a similar type of heating.

[4] A slightly smaller or bigger jet does not alter the global evolution (see G11).

Table 1. Parameters and properties of the most relevant models.

Model	Feedback	Efficiency (ϵ)	Notes
CF	No AGN heating	–	–
Bc1em2	Bondi	10^{-2}	Continuous
Bc5em2	Bondi	5×10^{-2}	Continuous
Bc1em1	Bondi	10^{-1}	Continuous
Bi1em3	Bondi	10^{-3}	Cold timing
Bi1em2	Bondi	10^{-2}	Cold timing
Bi5em2	Bondi	5×10^{-2}	Cold timing
Bi1em1	Bondi	10^{-1}	Cold timing
C5em5	Cold	5×10^{-5}	–
C1em4	Cold	10^{-4}	–
C5em4	Cold	5×10^{-4}	–
C1em3	Cold	10^{-3}	–
Int510l	5–10 Myr cycle	–	$P_{\rm j} = 10^{-5} P_{\rm Edd}$
Int510m	5–10 Myr cycle	–	$P_{\rm j} = 10^{-4} P_{\rm Edd}$
Int510h	5–10 Myr cycle	–	$P_{\rm j} = 10^{-3} P_{\rm Edd}$
Eth50	Thermal (+ Bc)	5×10^{-3}	50 per cent $E_{\rm th}$
IO1-9	InOut (+ Bc)	10^{-3}	$\dot{M}_{\rm in} = 0.1 \dot{M}_{\rm acc}$
IOen40	InOut (+ Bc)	5×10^{-3}	$40 \dot{M}_{\rm out}$ (IO3-7)
IOen80	InOut (+ Bc)	5×10^{-3}	$80 \dot{M}_{\rm out}$ (IO3-7)

In the Bondi feedback, the outflows are triggered by the usual prescription

$$\dot{M}_{\rm B} = 4\pi (G M_{\rm BH})^2 \rho_0 / c_{\rm s0}^3, \tag{8}$$

where ρ_0 is the volume-weighted hot gas density calculated within $\sim$2.5 kpc, while $c_{\rm s0}$ is the mass-weighted sound speed in the same region. The assumed supermassive BH has a mass of $3 \times 10^9\,{\rm M}_\odot$. The outflow energy is then calculated with equation (7), using $\dot{M}_{\rm B}$ instead of $\Delta M_{\rm cool}$. Needless to say, the Bondi radius, $r_{\rm B} \sim 80\,{\rm pc}$, is smaller than our resolution limit, so we refrain to attach a strict physical meaning to $\dot{M}_{\rm B}$. In this sense, the high mechanical efficiencies adopted for Bondi models are due to the fact that the accretion should be considerably larger (because of higher inner ρ_0 and lower $c_{\rm s0}$).

Besides the two main feedback schemes, we experimented some variations in the AGN generation, such as fixed intermittency, thermal feedback and direct linking between the outflowing and accreting masses. These special models are often not successful and they will be briefly explained through Sections 3.4– 3.6 (see also Table 1 for a summary).

For most of the presented methods, we applied injection directly in the domain with $M_{\rm act}$, as stated above. In other simulations, we tested also the injection of mass, momentum and energy flux through a 'nozzle' in the grid boundary at $z = 0$. This way the jet power is expressed as

$$\frac{1}{2}(\rho_{\rm jet} v_{\rm jet} A_{\rm n}) v_{\rm jet}^2 = \epsilon \dot{M} c^2, \tag{9}$$

with a nozzle area $A_{\rm n}$ of 2×2 cells and $\rho_{\rm jet} \sim 0.1$ the initial central gas density. We fix the temperature of the jet to very low values, compared to the IGM, in order to keep injected thermal energy at negligible levels compared to the kinetic flux.

As noted also in G11, the results do not greatly depend on the method of injection. However, the physical approach is a bit different: in the $M_{\rm act}$ method, we are directly modelling the entrainment, while in the nozzle injection, we are specifying the properties of the 'subgrid jet'.

3 RESULTS

In this section, we report the results of various simulations, exploring different types of feedback and parameters. We have analysed in detail the long-term behaviour of models similar to the most successful ones in G11. Some of the properties of unsuccessful – but pedagogical – models are covered in G11.

We stress again that the main objective of this work is to investigate the global properties of the flow, such as cooling rates and azimuthally averaged profiles (density, temperature, etc.). Cavities, shocks and iron abundances will be studied in depth elsewhere through a dedicated set of simulations at higher resolution.

3.1 Pure cooling flow

As a fiducial model, we ran a simulation without AGN feedback, that is, a pure CF. The results are shown in Fig. 1.

The flaws of the classical CF model are clearly depicted in this evolution. Both the density and (mass-weighted) temperature profiles steepen considerably in the central region: the radiative losses induce a subsonic inflow of the gas, increasing the emissivity in a vicious cycle. This trend is relatively more evident and fast in the galaxy group, rather than in the cluster. After just 1 Gyr, the cooling rate has already approached a quasi-steady state, with an asymptotic value $\sim 25\,{\rm M}_\odot\,{\rm yr}^{-1}$. This is the clearest discrepancy with observational data and one of the main failure of the standard CF scenario.

The other two main observables, $T(r)$ and $n_{\rm e}(r)$, are also clearly wrong in the inner $\sim$15 kpc (see Sections 1 and 2.1 for the observational references). Very cold gas, down to 10^5 K (which is soon dropped in our simulation), concentrates in the nucleus and generates non-consistent gradients. Our feedback models have to reduce this steepening, but preserving the cool-core appearance at the same time. As said in Section 1, galaxy groups present a more variable inner temperature profile with respect to clusters. Nevertheless, the heating must not destroy the inner structure (see also Brighenti & Mathews 2002, 2003), a quite demanding requirement.

A typical signature of such a strong CF is also the temporal increase in the bolometric X-ray luminosity: from $\sim 1.9 \times 10^{43}$ up to $\sim 2.6 \times 10^{43}\,{\rm erg\,s}^{-1}$ at 7 Gyr.

It is interesting to investigate the global energetic budget, because the common (misleading) sense would probably associate the irradiated energy with, mainly, the drop in internal energy. However, the internal energy within $r_{\rm vir}$ decreases by $\sim 7 \times 10^{58}$ erg (that is, by less of 1 per cent), while the potential energy drops by $\sim 6 \times 10^{60}$ erg, considering both the hot gas remaining in the grid and the cooled gas at the centre of the cluster. The kinetic energy stays always around $\sim 10^{57}$ erg and is therefore negligible. The conclusion is that energy is radiated away ($E_{\rm rad} \sim 6 \times 10^{60}$ erg in 7 Gyr) mainly at the expense of the potential energy of the IGM. This behaviour was less evident in the cluster, but still present.

In order to test the effect of numerical resolution on the CF results, we calculated a CF simulation with a resolution three times higher: the results are almost identical to the lower resolution run described above. Therefore, with the adopted resolution, our models are clearly in the convergence limit.

After placing the frame of the requirements for a successful feedback model, in the following, we will describe the simulations with heating linked to AGN outflows. In the next section, we will begin with the two best Bondi models and then we will discuss, from higher to lower efficiencies, computations with worse results, alternating the continuous and intermittent types of feedback.

3.2 Bondi feedback (or entropy-regulated)

3.2.1 Model Bc5em2, $\epsilon_B = 5 \times 10^{-2}$

We begin to analyse the results of the simulations with AGN feedback turned on.

The Bondi accretion theory (Bondi 1952), although highly idealized with respect to the complexity expected in real accretion systems, has been widely used to estimate accretion rates on supermassive BHs, adopting equation (8).

Despite our resolution is far from capturing the effective Bondi radius (tens of pc) and despite the fact that the radiative cooling is important in the central region, we think that Bondi accretion is still a useful, simple feedback prescription. In fact, the accretion rate is simply proportional to $K^{-3/2}$, where $K = T/\rho^{2/3}$ is the entropy parameter. Thus, Bondi regulation is intrinsically a good 'thermostat': when the gas is cold and dense, the feedback is stronger, and vice versa.

The first good model that we obtained is Bondi accretion with efficiency $\epsilon = 5 \times 10^{-2}$ (Fig. 2, second column), using the 'entrainment' injection in the active region. The zone for the weighted quantities is ∼2.5 kpc. The overall feedback is gentle and moderate, exactly as speculated.

The mean cooling rate is well below 10 per cent of the pure CF, with only a transient peak (∼3.5 $M_\odot$ yr^{-1}) at 1.5 Gyr. An important feature for a successful continuous feedback, as seen in G11, is stability in time. The moderate power stays around 10^{44} erg s^{-1}, without strong variations, which allows to balance the instantaneous cooling rate in an efficient way.

The mass-weighted temperature profiles are in agreement with observations in the nucleus of the group, with a smooth and almost flat curve. In the outer regions, tiny acoustic oscillations are present, while between 10 and 30 kpc the continuous injection of energy tends to slightly overheat this region, especially at late times. The density profiles also show little variation from the initial observed ones, an indication that the gas is not accumulating and peaking in the core.

Another relevant consideration is that the Bondi rate is always sub-Eddington (between 10^{-3} and 10^{-2} Eddington rate). Observations of X-ray bright elliptical galaxies (e.g. Allen et al. 2006) also point towards similar values.

The final injected energy is relatively low, $\sim 1.8 \times 10^{61}$ erg (3.6×10^{61} erg for the bipolar outflow), compared to the total 'available' BH energy 1.8×10^{62} erg, roughly estimated as $E_{BH} \sim 0.1 M_{BH} c^2$, with $M_{BH} = 10^9$. This will be a typical feature of galaxy groups, in contrast to the high input energies of massive clusters, whose models can sometimes exceed the above quantity.

Furthermore, we tested several initial conditions and we concluded that the dynamics and results of our feedback models are, overall, not distorted by relatively different initial temperature and gravity profiles. For example, in Fig. 2 (fourth column), we started the computation with an isothermal profile (∼1.35×10^7 K), retrieving the density structure from a theoretical Navarro–Frenk–White (NFW) plus deVaucouleurs potential. After the first Gyr of pure CF, the Bondi feedback ($\epsilon_B = 5 \times 10^{-2}$) is again very effective in quenching the CF and at the same time preserving the cool-core appearance.

A possible riddle for all continuous models remains the absence of frequent jet-inflated spherical cavities. The continuous AGN activity (mean $v \sim 10\,000$ km s^{-1}) carves a narrow tunnel of about 30 kpc in length, although its density contrast with the environment is large only for $z \lesssim 10$ kpc (and not particularly evident in the surface brightness maps; see Section 4).

3.2.2 Model Bi5em2, $\epsilon_B = 5 \times 10^{-2}$

In a self-regulated (subgrid) mechanism, we have to face substantially two problems. The first one is how much power to link to the feedback, while the second one is the right timing, that is, when to turn on and turn off the heating machine.

In the following simulation (Fig. 3, third column), we link the activation of the AGN heating to the gas cooling, but use the standard Bondi rate for the gas accretion on to the BH. In other words, an outflow is generated when $\Delta M_{cold} \neq 0$, with energy linked to $\dot{M}_B$ in the usual way.

This feedback scheme tries to reproduce a self-regulated intermittency of the outflows (ideal Bondi models can only be continuous), with cycles of inactivity corresponding to moments of high hot gas entropy. In fact, when the gas begins to cool, it will usually start to flow towards the central BH.

This way the temperature profiles are a bit more consistent with the observational data, especially at intermediate radii. Although the jets are intermittent, their frequency is high, a condition that grants the quenching of the cooling rate ($\dot{M}_{cool} \sim 0.5$–$2\ M_\odot$ yr^{-1}). The density profiles do not depart from the cool-core status, without a strong steepening (central values ∼ 0.1 cm^{-3}).

Bondi accretion rates are almost identical to Bc5em2, with the total energy injected in 7 Gyr being a bit less: $\sim 1.5 \times 10^{61}$ erg. The average jet power is also a factor of ∼1.3 less, $\sim 5.5 \times 10^{43}$ erg s^{-1}.

This model clearly solves the problem of jet-inflated cavities in the IGM. The outflow duty cycle[5] is roughly 80–85 per cent (in the whole computation). The pattern is not very regular; in fact, the cycle is more frenetic between 2 and 5 Gyr, when the central gas has been heated efficiently. Every time the jet (with velocities usually of 8000–10 000 km s^{-1}) turns on again, a bubble of small size (10–15 kpc) is seen in the density map. Note that after a period of quiescence the subsequent injection produces a peak in the power, promoting the above-mentioned cavity inflation through shock heating. The side-effect consists in more evident perturbations in some T profiles (e.g. 3 and 7 Gyr), however, still compatible with typical galaxy group observations.

Finally, during runtime, we calculated, at every time-step, the efficiency (ϵ_c) that would have the cold feedback mechanism (bottom panel). The result is striking: on average, the two schemes are almost coincident with ϵ_c around 10^{-3}, except for few short time-steps, in which the cold feedback requires 100 per cent efficiency (because the cooled mass is almost zero).

3.2.3 Model Bc1em1, $\epsilon_B = 10^{-1}$

We begin now to describe models from higher to lower efficiencies, alternating again continuous and intermittent Bondi methods.

The following simulation is computationally very expensive, because the (continuous) outflow velocity rises often over 20 000 km s^{-1}. It is shown in Fig. 2 (third column). The cooling rate is quenched to a fraction of $M_\odot$ yr^{-1} after just a few Gyr. The total injected energy is 3×10^{61} erg (about 1.5 times greater the intermittent counterpart, next model Bi1em1). The consequence of this high-energy deposition is a progressive steepening in the temperature gradient, with a moderate spike in the inner 4 kpc, where

[5] The common duty cycle retrieved by observations can be quite different from our numerical estimates, because the definition of an 'active' AGN highly depends on some luminosity threshold (in the X-ray, radio, etc.) and on the properties of the sample.

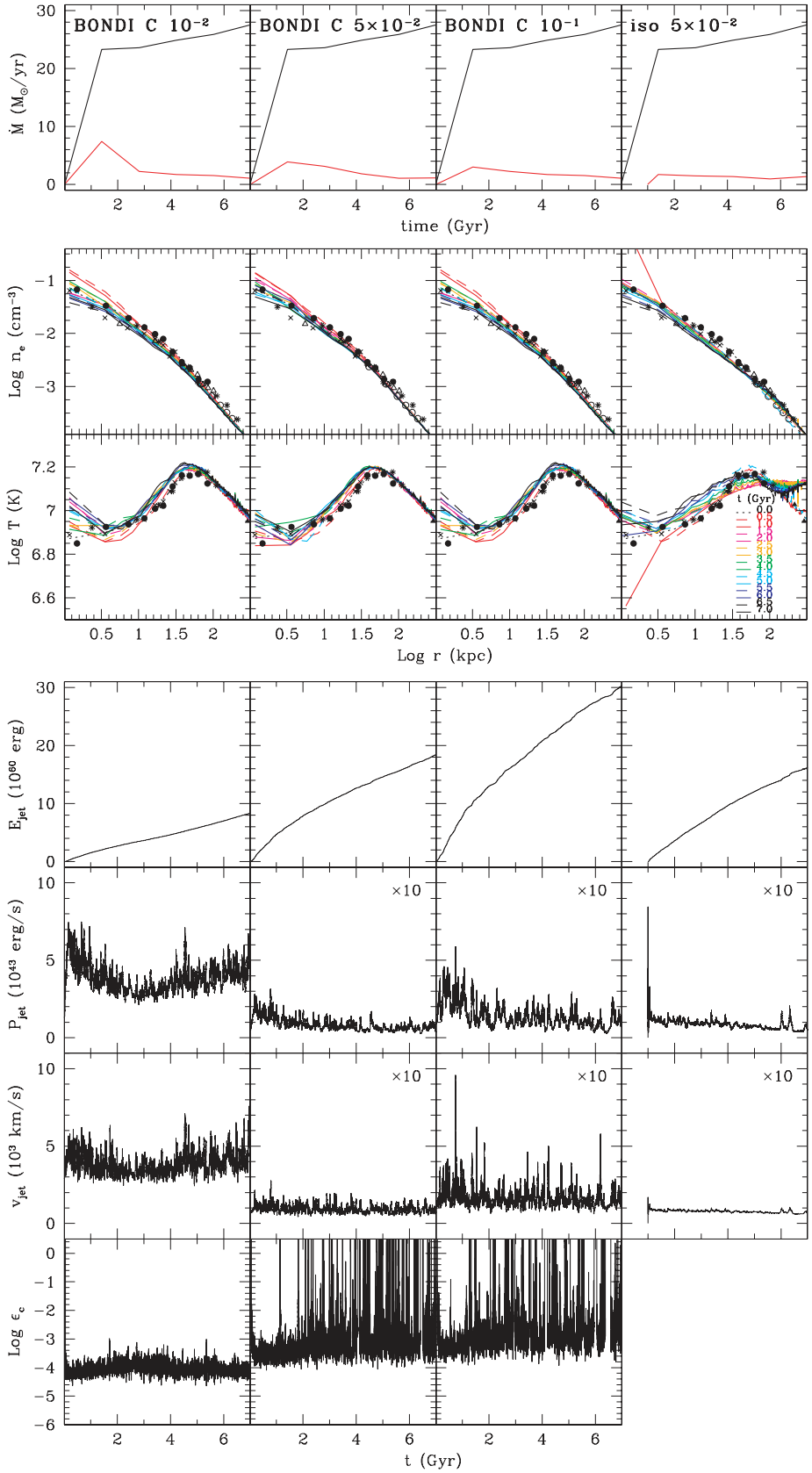

Figure 2. Evolution of Bondi (continuous) feedback models with different efficiencies (the latter being the isothermal start). The panels in the first three rows (top to bottom) represent the same quantities as in Fig. 1. The panels in the other four rows show the total injected kinetic energy (in the half-space $z > 0$), outflow power and velocity, and associated cold efficiency (see text). The label '$\times$ 10' means that the units in the ordinate axis have been multiplied by 10.

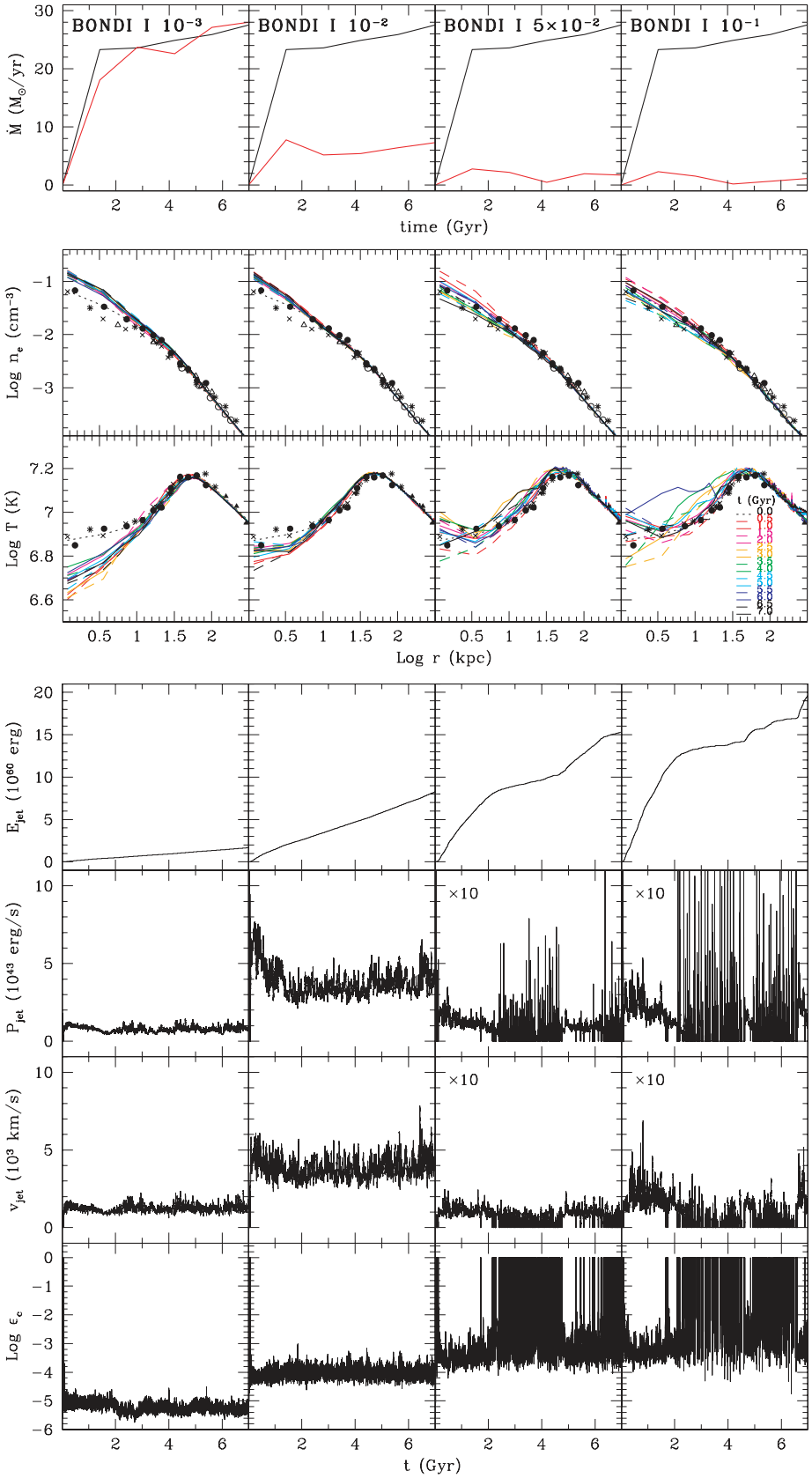

Figure 3. Evolution of Bondi (intermittent) models with increasing efficiencies, from the left-hand to right-hand side. The description of the plots are the same as for Fig. 2.

the jet is always active. During some time-steps the outflow reaches 5×10^{44} erg s^{-1}, a quite strong power for Bondi accretion.

The compared efficiency analysis (bottom panel) shows that a cold feedback triggering could not even be possible in 20–30 per cent of the evolution, because it would break the unity threshold. In the other periods, it would be associated with a value around 2.5×10^{-3}.

3.2.4 Model Bi1em1, $\epsilon_B = 10^{-1}$

The following (Fig. 3, fourth column) is another computationally expensive model, which touches the limit of acceptability in the parameter space, for Bondi models. The timing is again associated with the cold gas. The cooling rate is very similar to that of the precedent continuous model (Bc1em1), within the reasonable range 0.5–1.5 M$_\odot$ yr^{-1}, declining at late times. The density profiles are optimal, not altered from the initial data. Temperatures start to feel the strong outbursts, which have sometimes power in excess of 10^{45} erg s^{-1} (with velocity larger than 2×10^4 km s^{-1}). In fact, at later times, the central gas is heated up to 10^7 K, during some event.

The associated cold efficiency has a common trend around 2.5×10^{-3}, but with many oscillations after 3 Gyr reaches unity easily. Note that these moments last very few time-steps, after which ϵ_c reset to lower values (in contrast to a first impression of the tight plot).

3.2.5 Models Bc1em2 and Bi1em2, $\epsilon_B = 10^{-2}$

When the efficiency is lowered to $\epsilon = 10^{-2}$, the heating provided by the feedback is considerable ($\sim 8 \times 10^{60}$ erg). This decreases the cooling rate down to at least 30–40 per cent of that of the pure CF (Fig. 2, first column). The profiles are close to the observed data, thanks to an always continuous outflow with velocity (4–5) $\times$ 10^3 km s^{-1} and power (4–5) $\times$ 10^{43} erg s^{-1}.

The intermittent simulation is very similar to the continuous evolution (Fig. 3, second column), except that, initially, the system is permitted to cool. Without this early opposition, the outflows – with the same power – cannot halt the cooling so efficiently like in the previous case. The feedback finds an equilibrium only at 4 Gyr, while at later times, it will slowly increase, contrary to a reasonable self-regulated model.

The associated efficiency of a ΔM_{cold} model is near 10^{-4}. In fact, we will see that the linked cold feedback model will produce an almost identical outcome, that is, weak heating (Fig. 4, second column).

3.2.6 Model Bi1em3 (or Bc1em3), $\epsilon_B = 10^{-3}$

As a template for a typical weak model, a simulation with the Bondi efficiency of 10^{-3} produces a cooling rate, which is identical to a pure CF run: $\sim$25–26 M$_\odot$ yr^{-1} (Fig. 3, first column).

The only clue for the presence of AGN heating is that the profiles do not suffer a heavy decline with time, even if they possess a remarkable steep gradient (T down to 4×10^6 K).

The outflow is always continuous (the model could also be named as Bc1em3), with a very low velocity around 1000 km s^{-1} and a power often under 10^{43} erg s^{-1}. There is no possibility that this model will become intermittent at any time, due to the constant central cooling.

3.3 Cold feedback (ΔM_{cool}-regulated)

3.3.1 Model C5em5, $\epsilon_c = 5 \times 10^{-5}$

The results presented in the previous section for the Bondi accretion models suggest that, compared to galaxy clusters, groups require lower efficiencies of at least a factor of 10. Therefore, we start illustrating the cold feedback mechanism for the lowest adopted ϵ_c and then moving to more efficient outflows.

Here we still use the entrainment injection method, with the width and length of the active region 1 and 2 kpc (2 and 4 grid points), respectively. In G11, in fact, we concluded that the size of the jet and the type of injection do not change drastically the evolution of the feedback.

As shown in the first top left-hand panel of Fig. 4, the cooling rate settles on a steady value around $\sim$10 M$_\odot$ yr^{-1}. This rate is obviously unacceptable, although reduced to $\sim$50 per cent of the pure CF model value. With such a low efficiency, the azimuthally averaged, mass-weighted temperature and density profiles are only slightly modified by the heating and do present the excessive accumulation of gas near the centre, typical of the CF model. At the centre, the temperature is $\sim 5.6 \times 10^6$ K and the numerical densities $\sim$0.18 cm^{-3}.

The outflows, typically have a power of (4–5) $\times$ 10^{43} erg s^{-1} and a velocity of 3000–4000 km s^{-1}. The total injected mechanical energy is in fact quite low, 6×10^{60} erg, and the outflows are almost continuous, because they are never able to stop the CF. Given the rare period of inactivity, the 'duty cycle' is $\sim$95 per cent.

At the end of the simulation, 6×10^{10} M$_\odot$ has cooled and dropped out of the hot phase. The vast majority of gas cools at the very centre. If all the cooled gas were accreted on to the central BH, as we have simplistically assumed in this scheme, the final BH mass would result about an order of magnitude greater than the expected one. In principle, we could avoid the problem of the excessive BH mass by assuming that only a fraction of the cooled gas actually accretes on it with a higher efficiency (see Section 3.6, InOut models).

3.3.2 Model C1em4, $\epsilon_c = 10^{-4}$

As anticipated, the next step is to increase the efficiency, in order to find a more suitable heating power.

In the following model, where the efficiency is increased by a factor of 5, $\epsilon_c = 10^{-4}$, we obtain in fact a jet power of $\approx 10^{44}$ erg s^{-1} and velocity oscillating around 5000 km s^{-1} (see Fig. 4, second column). However, the cooling rate is only slightly reduced to 6–7 M$_\odot$ yr^{-1} and radial profiles tend to be similar to the ones of the previous model. The difference is that now the curves decline at 6 kpc, instead of 10 kpc. Evidently, the outflows deposit their energy in more inner zones.

We conclude that, even if the total injected energy reaches almost 10^{61} erg, at this stage, the CF is not quenched in a successful manner. This is also underlined again by the almost continuous presence of the outflows.

3.3.3 Model C5em4, $\epsilon_c = 5 \times 10^{-4}$

At 5×10^{-4}, we finally recover a successful heating evolution. As in previous computations, at early time (first Gyr), the radiative cooling prevails over the outflow mechanical heating and the cooling rate reaches a peak of 4 M$_\odot$ yr^{-1}. However, the long-term evolution presents different intriguing results. After 2 Gyr, the system

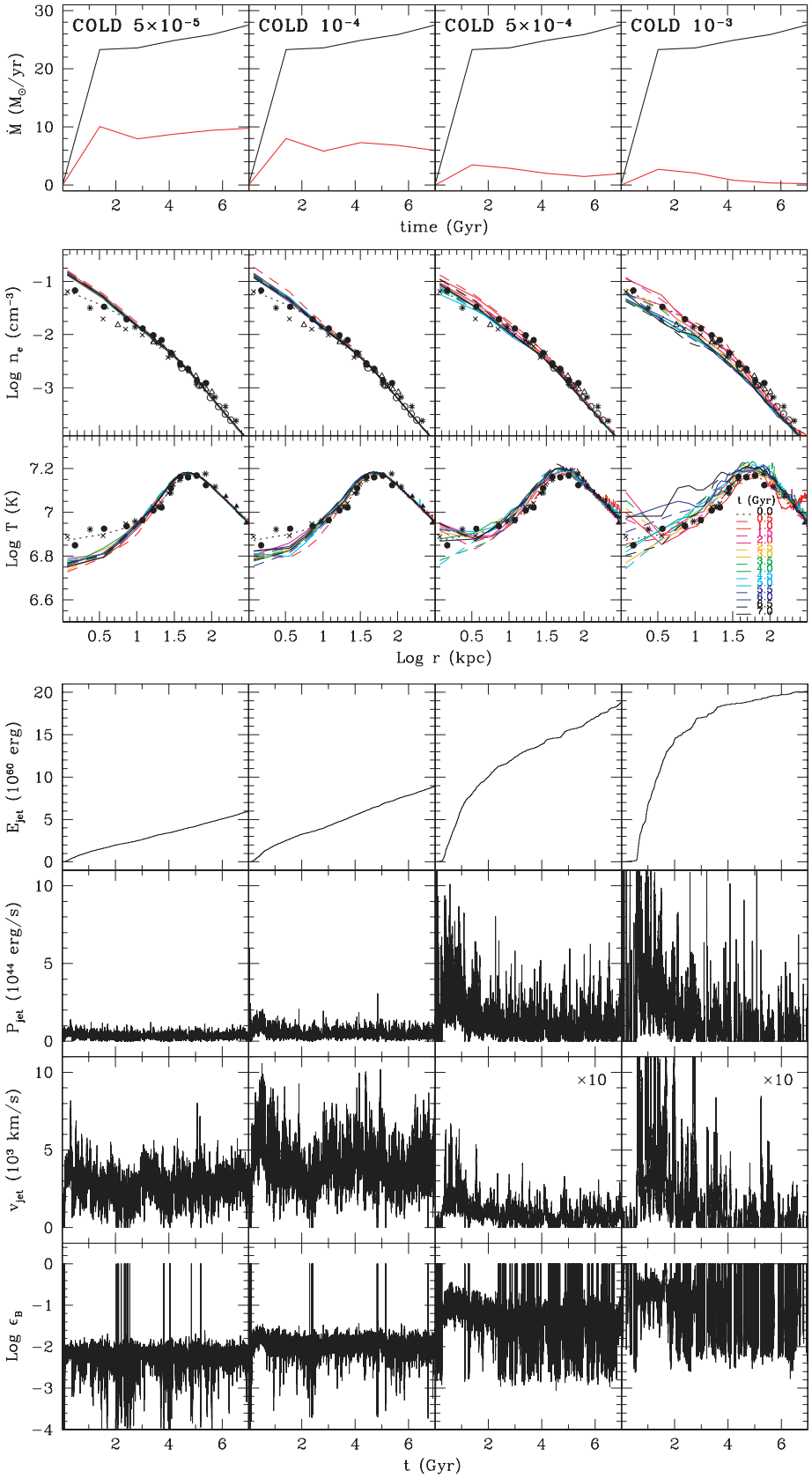

Figure 4. Evolution of all cold accretion models with increasing efficiencies, from the left-hand to right-hand side. The description of the plots are the same as for Fig. 2.

becomes much more turbulent and chaotic, inducing a reasonable amount of mixing, that permits gas circulation and reheating in a very efficient way, also in the 5-kpc nucleus.

As shown in the third column of Fig. 4, the temperature in that region is almost constant, with values close to that observed for NGC 5044 ($\approx 8 \times 10^6$ K; Buote et al. 2003; David et al. 2009). This very important feature is also described by the density curves: a gradual flattening of the central profile is seen through the entire evolution. It is striking that the 7-Gyr (black) profile is practically superposed to the initial fit. At that time (redshift = 0), the cooling rate is $\sim 2\,M_\odot\,yr^{-1}$, about 7 per cent of the pure CF run, a significant suppression which brings the value of $\dot{M}_{cool}$ in reasonable agreement with the observations (Buote et al. 2003; Tamura et al. 2003; David et al. 2009).

The shock waves generated by the outflows, with power usually in the range $\sim(2–5) \times 10^{44}\,erg\,s^{-1}$, are not strong enough to significantly alter the global positive temperature gradient, although small amplitude ripples are present. These waves correspond to weak shocks associated with the jet propagation and are visible up to a distance of $\sim$300 kpc. They are not so evident as in galaxy clusters because the energy involved here are two or three orders of magnitude lower. In fact the total jet energy is 1.8×10^{61} erg. The gas is typically ejected with $v_{jet} \sim 10^4\,km\,s^{-1}$.

Furthermore, an important difference between clusters and groups is the duration of each event. In cluster models, a duty cycle of 0.1 was quite usual, because the very short super-Eddington bursts could stop instantly the CF, with the consequence of perturbed profiles, near the ignition time. Here, our estimated duty cycle is roughly 0.85. Therefore, the situation is reversed: successful cold feedback models in groups require an almost continuous heating, with short pauses of tens of Myr.

Note that the Eddington luminosity $L_{Edd} \approx 1.5 \times 10^{38}(M_{BH}/M_\odot) \sim 10^{47}$ erg (for a 10^9-$M_\odot$ BH) is far above the regime of the current model. In fact the accretion rate oscillates between 10^{-3} and 10^{-2} the Eddington rate. As seen in Section 3.4, an L_{Edd} jet can easily erase the cool-core structure of the group.

In summary, the analysed behaviour of C5em4 seems to be similar to that the quiet Bondi feedback. In the bottom panel, we have calculated, at every time-step, the associated Bondi accretion rate and the required ϵ_B to reproduce the same instant mechanical energy. As a striking result, a Bondi efficiency of $\sim 5 \times 10^{-2}$, especially after 2 Gyr, is retrieved from this analysis. Only in a few events, the cold mechanism detaches from the regular regime of Bondi, because of its intrinsic impulsivity. Nevertheless, the similitude is quite evident and indeed, if we compare the two outcomes of both models (especially intermittent Bondi, Fig. 3, third column), they appear deeply connected also in a quantitative manner.

3.3.4 Model C1em3, $\epsilon_c = 10^{-3}$

Increasing the efficiency by a factor of 2 generates another positive model, with some features approaching the borderline of a violent disruptive heating.

In fact, with a jet power up to $10^{45}\,erg\,s^{-1}$, the CF is perfectly stifled, asymptotically decreasing to a fraction of $M_\odot\,yr^{-1}$ after a few Gyr (Fig. 4, fourth column).

The beginning of the violent regime is quite evident in the averaged profiles, which now tend to oscillate in a large $\sim$50 kpc region. Overall, the cool core is conserved, but the temperature indicates some overheating in the nucleus at later times.

With our adopted active region, in a few outbursts, the velocity is greater than the $10^5\,km\,s^{-1}$ line, while the outflow mass rate is several tens of $M_\odot\,yr^{-1}$, as in all previous ΔM_c models. This is a clear indication that at higher efficiencies we will approach a relativistic regime and a catastrophic heating (we will not show here results for $\epsilon_c > 10^{-3}$ but see fig. 5 of G11 for an analogous model for clusters). The equivalent Bondi efficiency for model C1em3 is sometimes 0.5 or more, difficult to justify.

The total injected energy of model C1em3 is similar to that of he previous successful model, a sign of a good self-regulation in the global feedback process. This energy can be compared with the total energy radiated away, $\approx 1.38 \times 10^{60}$ erg (in the simulated half-space $z > 0$). Interestingly, the present heating provides more energy than that lost by radiation ($E_{rad} \sim 1.4 \times 10^{60}$ erg). Note that, in every described model, the total outflow energy (for the full-space system) is about an order of magnitude lower than the available BH energy ($\sim 1.8 \times 10^{62}$ erg). The evolution of the energetics is very similar to the description presented by G11. The core kinetic energy increases after every intense AGN outburst, but it is soon dissipated and transformed into potential energy through the expansion of the IGM.

3.4 Intermittent feedback

3.4.1 Model Int510m: $10^{-4}P_{Edd}$

In this series of models, we want to decouple the simulation from the self-regulation engine, in order to control some important AGN outburst parameters. For example, it is interesting to fix the frequency of the outflows. In G11, we found that intermittent outflows, with the jet duration of 5 Myr and activated every 10 Myr, are very effective in inhibiting gas cooling by preserving the correct temperature and density profiles in galaxy clusters. This AGN activity cycle agrees with observations of acoustic 'ripples' in the Perseus cluster (e.g. Fabian et al. 2006).

In the models described in this section, we do not insert an ad hoc velocity, but we retrieve its value from setting a constant power, here taken equal to $10^{-4}P_{Edd}$. Thus, $P_{jet} \sim 4 \times 10^{43}\,erg\,s^{-1}$. We choose the 'nozzle' injection method; therefore, the velocity is constant: $7000\,km\,s^{-1}$. Note that the efficiency is irrelevant in the computation.

As a result (Fig. 5, first column), the cooling rate is less than a few $M_\odot\,yr^{-1}$, for several Gyr, and shows a slow increase after 4.5 Gyr, up to 4 $M_\odot\,yr^{-1}$. The azimuthally averaged density profiles are almost superposed to the observations, with a slight decrease in time, becoming flatter.

Thus, like in Bondi models, the radiative cooling is significantly reduced by the simulated heating process. Using the nozzle injection (essentially an outflow with negligible height) produces a spike in the very few kpc, while at radii greater than 10 kpc, the fluctuations from initial $T(r)$ are almost zero. As expected, shock heating is more vigorous in the nucleus when the outflow is injected through the boundary, while more effective at intermediate radii, when the entrainment method is adopted.

In this type of intermittent models, it is not granted that the feedback produces evident cavities. In fact, with a cycle of 5–10 Myr, the head of the jet cocoon almost touches the backflow tail of the last bubble. Thus, we expect that with a duty cycle greater than 50 per cent the jet becomes practically continuous.

3.4.2 Model Int510h/l: 10^{-3} and $10^{-5}P_{Edd}$

Keeping the same cycle scheme (5–10 Myr), but increasing the power by a factor of 10, produces a typical 'exploding' simulation

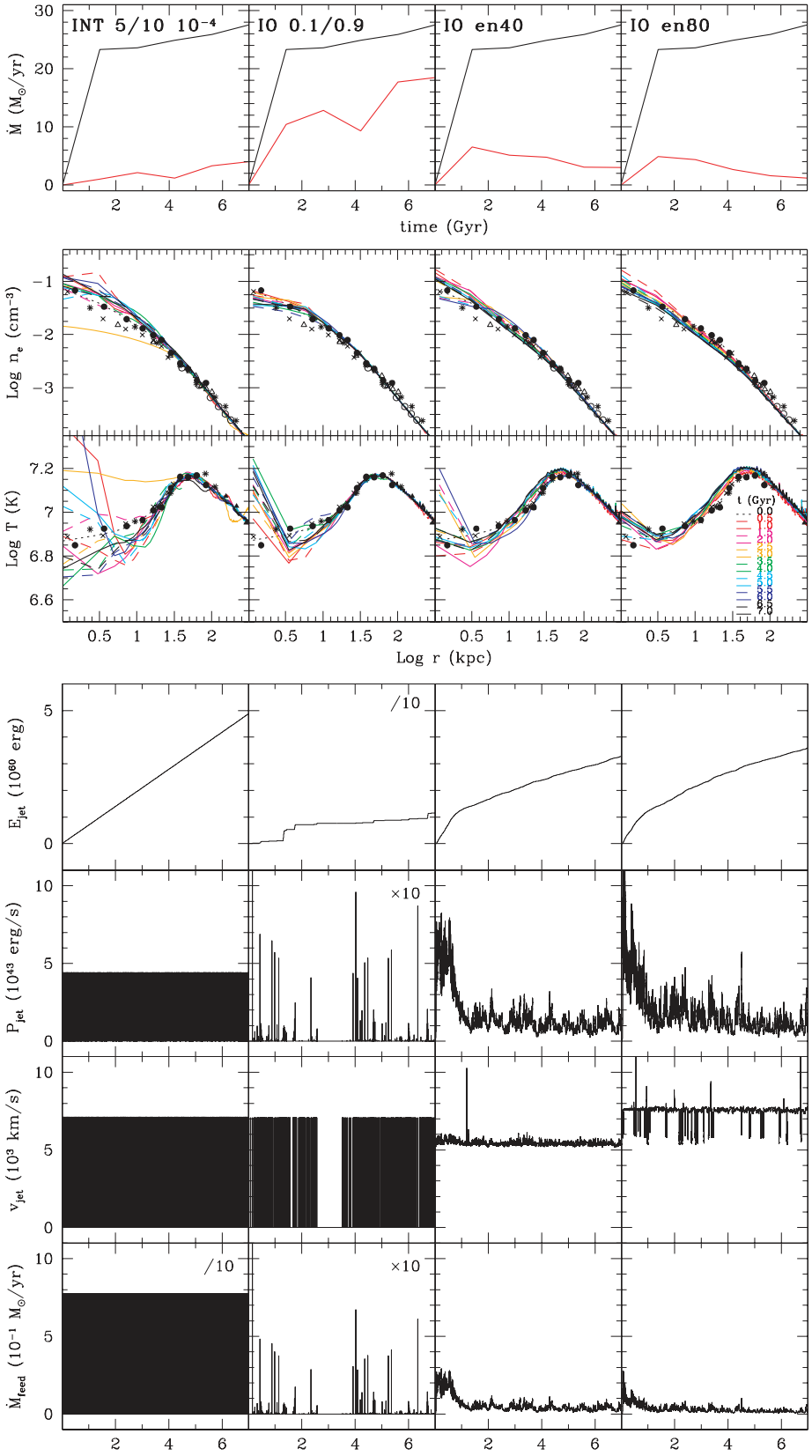

Figure 5. Evolution of intermittent and InOut models (with or without mass loading). The description of the plots is the same as for Fig. 2.

(not shown). The temperature profile gets a very steep negative gradient, as soon as the outflow ignites, destroying the entire cool core and generating a 'plateau' in $n(r)$. The cooling rates are obviously zero, but with unacceptable observables.

On the other hand, with a much lower power (4×10^{42} erg s^{-1}) $\dot{M}_{\rm cool}$ approaches 12 M$_\odot$ yr^{-1} after just 1 Gyr. Generated bubbles are quite stable and, being slowly inflated, show cold rims in the early phases. Nevertheless, the density and temperature profiles resemble those of a classical CF, with less peaked gradients.

We can conclude that, even with fixed intermittency, an acceptable AGN feedback model should not approach an Eddington regime (like proposed in some analytical works, e.g King 2009), at least in galaxy groups, where a strong burst can easily wreck the delicate thermodynamic structure of the core.

3.4.3 Varying fixed cycle: 1–10, 2.5–10, 3.3–10, 7.5–10

Keeping a fixed jet power, as in our acceptable model Int510m, but this time varying the duration of the AGN activity, leads to models that must be rejected.

Indeed, when every outflow event has a duration of 1, 2.5 or 3.3 Myr, the intermittent feedback becomes quite ineffective in halting the inflowing cold gas: the central gas density slowly grows with time until radiative cooling prevails over heating, causing the cooling rate to surpass the threshold of acceptability. For example, after just 1 Gyr, with 3.3 Myr duration, the cooling rate is over 7 M$_\odot$ yr^{-1} and the temperature curve turns very similar to those of model CF.

On the contrary, when the jet duration exceeds 5 Myr, the inflated cavities disappear, because the different outbursts melt rapidly in a 10-kpc zone, producing an almost continuous injection. The consequence is a steep T gradient at the centre, which can halt the CF, but without self-regulation it easily overheats the system.

3.5 Thermal feedback

3.5.1 Adding thermal energy: 20 per cent up to 99 per cent

It is worth noting that one difficulty of a pure kinetic outflow (often called 'momentum-driven') is that it can easily carve a tunnel in the surrounding IGM if the ram pressure of the jet ($\rho_{\rm j} v_{\rm j}^2$) is much larger than the thermal pressure ($\rho c_{\rm s}^2/\gamma$) of the gas. Thus, a feedback with high kinetic energy will advance undisturbed in the group core, depositing its energy at intermediate radii (15–30 kpc). At the base, the cold gas accumulates in a torus-like manner. This is especially evident at early stages of a momentum-driven outflow. The successful models, we found, are able to quench the CF, because at some point the generated turbulence induces strong mixing in the gas, also at the very centre. Therefore, the circulation inside the jet path makes shock heating very effective. In our models, the turbulence is sustained only by the AGN feedback. It is likely that this process dominates in the very central region of the system, although turbulent and bulk motions caused by cosmological accretion, usually very subsonic, may also contribute (e.g. Heinz et al. 2006).

Nevertheless, the high-density gas in the torus cools efficiently and triggers the AGN feedback in an almost continuous way. It is physically reasonable that a part of the jet power is converted into thermal energy, especially during the entrainment process. Based on these considerations, we simulated some models with a fraction of the total injected energy in the form of thermal energy, through the nozzle. We kept the Bondi prescription for the feedback method.

As a pedagogical purpose, we first set the fraction of $E_{\rm th}$ as 99 per cent of the total energy. This setup is similar to the model of Cattaneo & Teyssier (2007) with a loading factor of 100 and Bondi efficiency 0.1. As expected, the first powerful outflow (over 10^{44} erg s^{-1}) destroys the entire thermodynamic structure of the cool core: the produced shock (with temperatures above 10^{10} K) is almost spherical. This is another indication that the group necessitates much more delicate heating compared to a cluster. Lowering the efficiency to 10^{-3} still generates similar catastrophic heating.

On the other hand, keeping the above efficiency, but reducing the fraction of $E_{\rm th}$ to 20 per cent or 33 per cent, results in models overall similar to purely kinetic ones. One major difference is small puffs at the base of the jet that enable more turbulence. The problem is that, in the inner 8–10 kpc, temperature profiles show a spike, due to injected $E_{\rm th}$. Another interesting effect is the enlargement of the tunnel carved by the outflow, because of the increased internal pressure, compared to the momentum-driven one.

The best model seems to be Eth50 (not shown), with 50 per cent thermal energy and efficiency 5×10^{-3}. The feeble jet is almost always continuous, with velocity 3000 km s^{-1}, but the thermal energy injection generates a break-up in the jet structure, which fragments in small buoyant bubbles of size 5–8 kpc; a very interesting feature that is seen in NGC 5044 (David et al. 2009, 2010).

We conclude that a good fraction of the thermal energy associated with the AGN feedback can help in the deposition of heating at very small radii, reducing the cold torus at the base of the jet and fragmenting the outflow in small-size bubbles. At the same time, however, it is difficult to obtain a flat or positive (mass-weighted) T profile. We will expand this analysis in a future work, with very high resolution.

3.6 In and out feedback

3.6.1 Model IO1-9

One problem of self-regulated feedback models is how much of the gas contributes to the growth of the BH mass. Needless to say, with a resolution of ∼500 pc, we cannot consistently estimate the accretion rate on to the BH. As noted in some works (e.g. Cattaneo & Teyssier 2007; Ostriker et al. 2010; G11) part of the inflowing gas on to a BH could be thrown back by the generated outflow, perhaps through entrainment. Therefore, only a fraction of the accreting mass, $\Delta M_{\rm acc}$, might actually be captured by the BH. From another perspective, we can see this as a reduced total efficiency.

That being stated, we computed some models in which we attempt to track the part ($f_{\rm in}$) of the infalling gas that really increases the BH mass. The residual fraction ($f_{\rm out} = 1 - f_{\rm in}$) is considered the active mass of the outflow:

$$\frac{1}{2} f_{\rm out} \dot{M}_{\rm acc} v_{\rm jet}^2 = f_{\rm in}\, \epsilon \dot{M}_{\rm acc} c^2. \quad (10)$$

Note that in these models it is better to use the nozzle injection mode, in order to totally control the outflowing mass, without altering the internal domain.

An interesting feature of this method is that the outflow velocity is practically constant, dependent on $f_{\rm in}/f_{\rm out}$ (and ϵ). An observational constrain of the outflow velocity may thus give hints about this ratio between infalling and outflowing matter.

Setting $f_{\rm in} = 0.1$ ($f_{\rm out} = 0.9$) and efficiency 10^{-3}, the outflow, coming out of the nozzle, has a velocity around 7000 km s^{-1}. With cold accretion, the power of the jet presents strong oscillations between 10^{43} and 10^{45} erg s^{-1}, while the cooling rate approaches in a few Gyr the pure CF simulation. Even with Bondi accretion (same efficiency; Fig. 5, second column), which, in theory, is more regular,

the (high) outflow power cannot find a stable balance in time, resulting in $\dot{M}_{\rm cool} \sim 18\,{\rm M}_\odot\,{\rm yr}^{-1}$ at 7 Gyr. While some accretion events reach 4–5 $\rm M_\odot\,yr^{-1}$, the produced strong feedback does not last long enough. In fact, the total injected energy is very low: 10^{59} erg. It is interesting that the radial profiles of this model (IO1-9) show a cool core, with the exception of a central negative temperature gradient. Therefore, overall acceptable mean T and n profiles do not necessary imply that the system is not cooling.

Trying to increase the efficiency is a serious problem for the InOut model, because the velocity will constantly overtake $50\,000\,{\rm km\,s^{-1}}$. We could lower $f_{\rm in}$ in order to increase the jet mass, but with just 1 per cent of the accreting mass (probably unrealistic) the velocity will still have very large values.

3.6.2 *Models IOen40 and IOen80*

The only solution, we have found, is to return back to the 'entrainment hypothesis' and multiply $f_{\rm out}$ by a factor η (like a mass-loading factor). Following this assumption, with $\eta = 40$ and $f_{\rm out} = 0.3$, we could enhance the Bondi efficiency ($\epsilon = 5 \times 10^{-3}$) to obtain an acceptable cooling rate, below 5 $\rm M_\odot\,yr^{-1}$ (Fig. 5, third column), after the small bump at 1.5 Gyr. Now the velocity has a value of $\sim$6000 $\rm km\,s^{-1}$. With $\eta = 80$, the average cooling rate is further reduced, asymptotically decreasing to 1 $\rm M_\odot\,yr^{-1}$ (fourth column). Both simulations generate some of the best radial profiles, which keep the cool-core appearance for the entire evolution time, almost 'glued' to the initial (observed) condition. This is an indication that the feedback has returned stable [around $P_{\rm j} \sim (1\text{–}3) \times 10^{43}\,{\rm erg\,s^{-1}}$], gentle and continuous, very similar to successful Bondi models (Section 3.2). Note that the accretion rate is again sub-Eddington.

Overall, a pure InOut model exhibits a spasmodic behaviour, because of the intrinsic linking between accreting and outflowing matter, which can be smoothed out only by introducing a mass-loading factor. However, this parameter is nowadays unknown and therefore its value is chosen ad hoc, in order to retrieve reasonable jet velocities. It is therefore simpler and cleaner to adopt the usual entrainment feedback of the main models (Sections 3.2 and 3.3), seeing that the results are analogous.

4 DYNAMICS AND OBSERVABLES

In this section, we will show the 'real face' of the best simulated models, at some relevant times. We will analyse physical quantities, such as gas density, and other astronomical observables, that is, integrated emission-weighted maps. Note that the entire structure of our computation favours the study of a very long term evolution. In order to fully comprehend the dynamics of single-burst events, we should carry on a short-term evolution with much higher resolution. We will confront this setup in a future dedicated paper.

In Fig. 6, the first column exhibits 2D density cuts through the x–z mid-plane (panels a–d) with the velocity field superposed. The first row is associated with model Bc5em2 (at 5 Gyr), one of the successful models in our set of simulations. This snapshot depicts one of the three typical stages of the AGN-regulated simulation in a galaxy group. The gentle and continuous heating of the outflow ($\sim 10^{44}\,{\rm erg\,s^{-1}}$) carves a narrow tunnel in the IGM with electron density around $2 \times 10^{-4}\,{\rm cm^{-3}}$. The diameter of the channel is usually 4–5 kpc, collimated in the inner region by the thermal pressure of the surrounding gas. At 14 kpc, where the jet ram pressure becomes comparable to the thermal pressure of the ambient gas ($P_{\rm th} \sim 2.5 \times 10^{-11}\,{\rm erg\,cm^{-3}}$), the outflow structure becomes perturbed and more turbulent.[6] In fact, near the tunnel, instabilities are visible, a signature of further IGM entrainment and turbulent mixing. The latter has a relevant role in the feedback process, especially at later times, when the AGN has been active for several Gyr (Fig. 2, cooling rate decreases with time). In fact, even if the turbulent mixing does not directly heat the gas, it greatly favours the deposition of energy at the base of the jet, where the cooling tends to dominate.

The fact that the global cool-core appearance is not greatly modified is another key result. Although the continuous outflow generates a tunnel, the overall initial structure is conserved. On the other hand, increasing the efficiency of Bondi models leads to a wider V-shape channel, which begins to dominate the core of the group. This is not observed and in fact those models are rejected also for the central negative T gradient. As seen in the second column (panel e), the (emission-weighted) temperature of model Bc5em2 has instead a positive gradient, almost flat in the 5-kpc nucleus.

The continuous presence of the channel (interrupted sometimes by the fragmentation) is a feature not commonly seen in real groups, at least in the local Universe.[7] However, in the third column (panel i), the X-ray surface brightness map does not show an evident channel, with only two very faint features (at 12–16 kpc), similar to a pair of 'arms'. Going into quantitative details, we performed 1D cuts through z of $\rm SB_X$ at different levels (from 4 up to 20 kpc; see Fig. 7, non-black lines). It is clear that the central depressions are not deep (15–20 per cent, usually with a difference of $5 \times 10^{-6}\,{\rm erg\,s^{-1}\,cm^{-3}}$), plus the width is particularly slim (few kpc), making the detection of the channel extremely difficult.[8] Over 20 kpc, the slim tunnel is lost in the integration trough line of sight.

The last column is associated with the tracer of the iron abundance (again emission-weighted), injected by SNeIa and SWs of the cD galaxy (see G11 for details). This type of advected quantity is deeply linked to the history of the AGN heating. In panel (o), it is indeed possible to recognize the outflow pattern, which is asymmetrical and can drag the metals produced deep inside the central elliptical galaxy up to 15–20 kpc, with values around 0.3–0.4 $\rm Z_\odot$. This characteristic is commonly observed in the core of AGN-heated systems (e.g. Kirkpatrick et al. 2009; Rasmussen & Ponman 2009; David et al. 2010; Kirkpatrick, McNamara & Cavagnolo 2011; Doria et al., in preparation).

The second row of Fig. 6 shows another good model, one based on the cold feedback. C1em3 (at 0.5 Gyr) shows the other face of the AGN-regulated evolution: an AGN burst with power $\sim 1.2 \times 10^{45}\,{\rm erg\,s^{-1}}$ generates a big cavity in the IGM density, with the major-axis/minor-axis of 16/10 kpc. The injected energy is almost 10^{60} erg, with an outflow velocity over $10^4\,{\rm km\,s^{-1}}$. The buoyant bubble has a high density contrast with the environment, $\sim$100.

In contrast to the violent cavities generated in our previous galaxy cluster simulations (G11), the cold accretion mechanism is able to inflate low-density cavities without heavy shocks. The outflow power is in the group simulations several orders of magnitude lower and the injection per time-step is usually smoother. In fact [see panel (f) and Fig. 7, black line of the bottom panel], $T_{\rm w} \sim 1.45 \times 10^7$ K inside the shell which is only slightly larger than the surrounding

[6] At 24 kpc, the outflow is almost stopped by the IGM, generating a rise in temperature, $\sim 1.55 \times 10^7$ K (see also Fig. 7).

[7] The evolution of groups is still far from being certain, lacking a complete sample at intermediate and high redshift.

[8] In addition, Poisson noise, background, resolution and the response of the X-ray detector (not present in our mock maps) could easily alter or obscure this very faint and narrow feature.

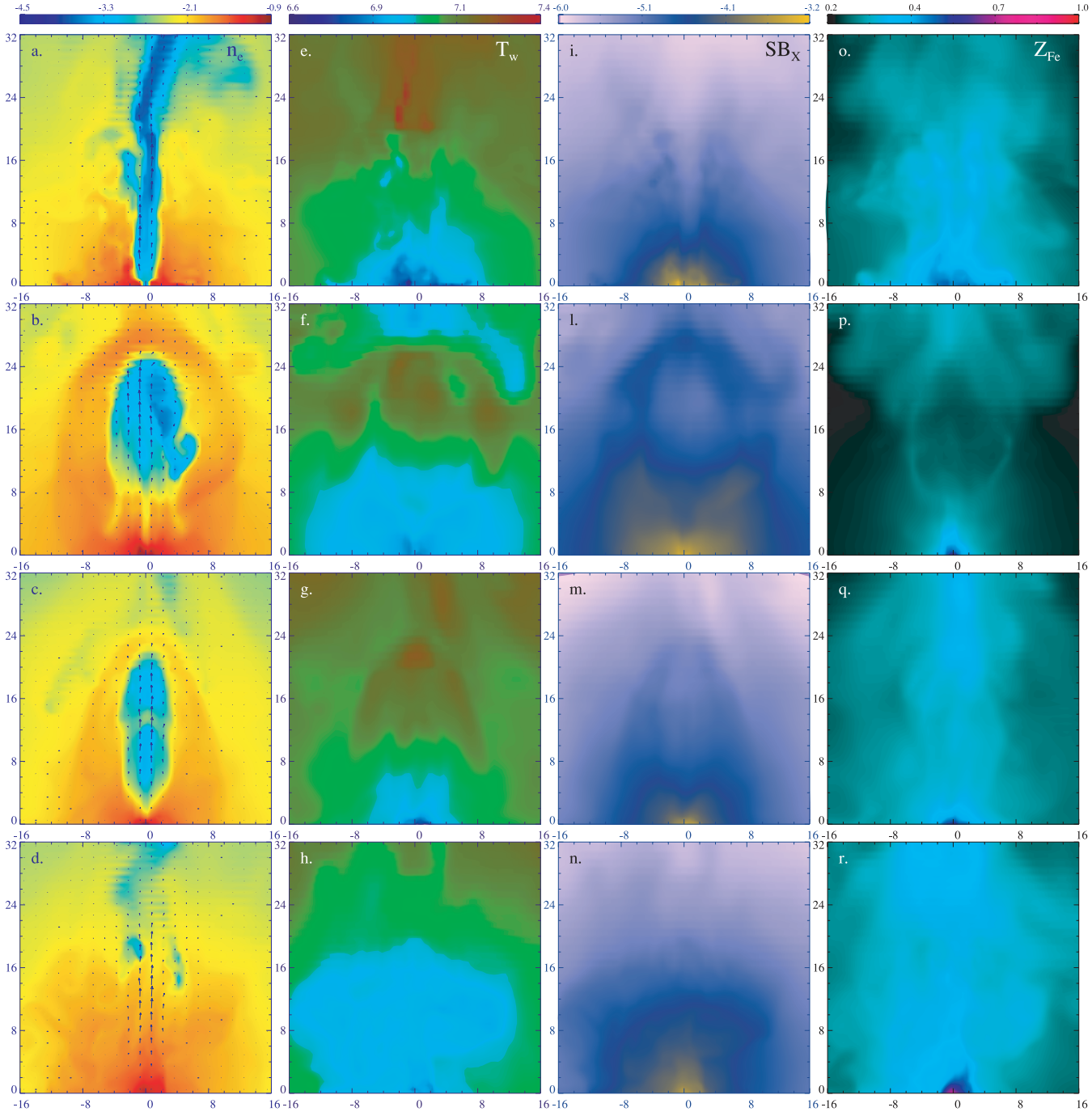

Figure 6. Maps of four best models (kpc unit). Columns (from the left-hand to right-hand side): cuts through the x–z mid-plane of the electron number density (cm^{-3}, logarithmic) with the velocity field superimposed; emission-weighted temperature maps (K, logarithmic); X-ray surface brightness maps (erg s^{-1} cm^{-2}); and emission-weighted iron abundance maps ($Z_\odot$ units). Rows (from the top to bottom) are associated with different models: Bc5em2 (5 Gyr); C1me3 (0.5 Gyr); Bi5em2 (7 Gyr); and Bi1em1 (6.5 Gyr). The colour scale is given by each bar at the top.

gas value. This is also suggested by the homogeneity of the map above 12 kpc (reddish colours).

A striking feature, usually hard to detect, is the bright rim that surrounds the cavity (panel l). The rim, especially the low-z region, is formed by low-entropy gas originally at the centre. This feature is often seen in deep X-ray observations (e.g. Salomé, Combes & Edge 2006, and references therein), suggesting that the rims are colder than the average ambient medium. The 1D cut through $z =$ 20 kpc (Fig. 7) clearly confirms the presence of this kind of rim, a drop in temperature (about 40 per cent) coincident with the high X-ray emission (at $x = \pm 6$ kpc).

In panel (p), we show the (emission-weighted) iron abundance map in the x–z plane. The iron-rich core, few kpc in size, is clearly visible. At $z \sim 28$ kpc, there is a region of Fe-rich gas, lifted by the outburst. The dense cavity rims also have a slightly larger abundance than the ambient gas, also revealing that the origin of a part of the rim material is connected to the nucleus of the group.

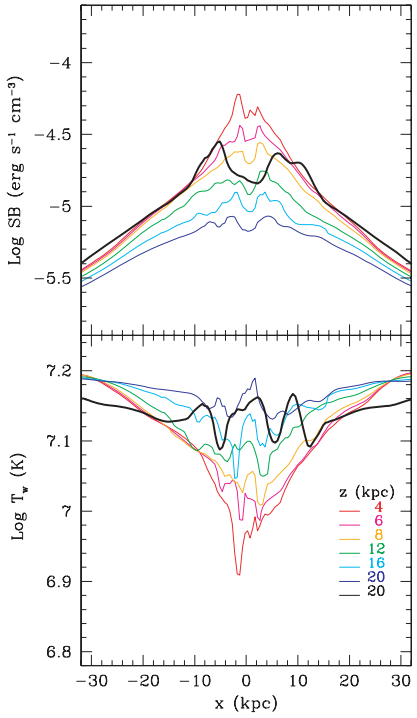

Figure 7. X-ray surface brightness and emission-weighted temperature 1D cuts through z (see legend). The black thick lines correspond to model Bi1em1 (panels n and h of Fig. 6), while the others belong to model Bc5em2 (panels i and e).

The SB_X inside the cavity (panel l) exhibits a depression of ∼50 per cent with respect to the rims. Note how this feature (Fig. 7, black line) would be easily detectable in the X-ray, compared to the vanishing faint channel, due to its deep depression and large width. Moreover, the nucleus (5–8 kpc) dominates the emission, while the upper part of the bubble vanishes rapidly in the background (>30 kpc). The future of this bubble is to buoy outwards and being destroyed, after few tens of Myr, by the backflow and instabilities.

The third row presents the snapshots of model Bi5em2 at 7 Gyr. At that stage of evolution, the IGM has accumulated more turbulence, after several AGN events, promoting the diffusion of iron in a radius of 20 kpc from the centre (panel q). However, this particular moment is again dominated by another AGN outburst (2×10^{43} erg s^{-1}). Therefore, the young bubble (panel c) still buoys undisturbed in the IGM, generating a slight asymmetry in the iron distribution along the jet axis, over the more uniform background.

At this time, we caught indeed the early injection phase of the outflow. A quasi-cylindrical cocoon envelops the core of the jet, which has now a velocity around 3000 km s^{-1}. The injected initial velocity was over 10^4 km s^{-1}, meaning that the jet commonly decelerates in a rapid way after few kpc. At $z = 22$ kpc the emission-weighted temperature reaches the maximum value of 1.62×10^7 K (panel g), clearly indicating the effect of shock heating. Around the contact discontinuity, the gas is weakly shocked, with temperatures above 1.25×10^7 K. The average Mach number is around 1.2, a typical value found by observations (Blanton et al. 2009; Gitti et al. 2010). The arc is also visible in the SB_X map (panel m), while the decrement associated with the cavity is ∼35–40 per cent.

Note that the maps of this model are very similar to those of model C5em4, another successful model, which has analogous bubble production. This behaviour confirms further the strict relationship between (intermittent) Bondi and cold models, as previously noted by the compared efficiency analysis.

The last row of maps displays another snapshot, typical for intermittent (self-regulated) feedback models, like Bi1em1. The big outburst and the generated bubble have been vanished, leaving the system in the aforementioned turbulent phase, in which mixing distributes the low residual heating to the central IGM. Soon after this period, the gas will cool and start the inflow. The velocity field is relatively chaotic (panel d), with the maximum velocity of 640 km s^{-1}, a bit lower than the local speed of sound, evidently decreasing in the turbulent zones. The mixing of gas at this epoch restores the spherical symmetry of the cool core, with the average temperature of $\sim 9 \times 10^6$ K (panel h). This is underlined also by the symmetric surface brightness map (panel n) and by the substantial diffusion of Fe in the intermediate zone, 10–30 kpc (panel r). Note that the abundance radial profile at the very centre is, however, more peaked during this quiescent CF phase (∼0.8 $Z_\odot$), compared to the AGN outburst period. Thus, our AGN models might also explain the dichotomy of cool-core and non-cool-core groups, the former having higher central abundances (Johnson et al. 2011).

An interesting feature, captured at this stage (often present after an AGN outburst), is the sequence of very small 'bubbles' at $r >$ 15 kpc, with a typical diameter of a few kpc. The origin of these tiny 'bubbles' is the fragmentation of the jet due to turbulent and chaotic motions, previously discussed. In this map, they are in a very late phase, almost disappearing in the ambient medium. In this case, they would be probably not detected in the X-ray (just a 10 per cent jump in surface brightness). To capture their signature, an observation should be done at an earlier evolutionary moment, after a big event, when the jet is rapidly collapsing. Nevertheless, it is striking that David et al. (2009, 2010) find exactly this type of configuration in NGC 5044: few big cavities and many small 'weather-driven' bubbles, which appear to be radio quiet (i.e. not directly inflated by the jet).

Overall, we conclude that the AGN outflow dynamics are particularly complex, as expected from the previous study in galaxy clusters. The main stages of evolution for the best models are (i) a gentle continuous outflow, which sustains the CF for the majority of time (or always in Bc models) and which is barely observable in SB_X maps; (ii) a phase of large cavity inflation, with cold rims and high density/SB_X contrast (only for non-continuous models); and (iii) small periods of quiescence in which the turbulence and vorticity promote mixing and tiny weather-driven 'bubbles'.

The presence of the above-described features (big and small cavities, asymmetry of Fe abundance, low Mach shocks, etc.) is consistent with several recent X-ray observations of heated systems and demonstrates the fundamental role of AGN-driven outflows in the evolution of groups (and clusters).

5 DISCUSSION

In this paper, we have proposed 3D numerical simulations of self-regulated AGN outflows in a galaxy group environment. We have followed the long-term evolution of the interaction between two main characters: radiative cooling and feedback heating. The aim of this work is to understand the general features of the feedback process to solve the CF problem, that is, quenching cooling rates, but, at the same time, preserving the global cool-core structure.

We tested two relevant models, which we had found to be successful in galaxy clusters (G11): cold feedback and Bondi feedback mechanisms. Galaxy groups, with masses approximately two orders of magnitude less than big clusters, are more fragile systems and

the feedback must be consequently more delicate. In the following, we discuss and summarize the main results obtained, along with merits and flaws of the models.

5.1 Hot continuous Bondi (Bc)

In the first set of simulations, the commonly adopted Bondi prescription is applied to evaluate the accretion rate on to the BH. Although the Bondi scenario is quite naive, it can be treated as the template model for typical self-regulated feedback directly linked to entropy. The efficiency, as a free parameter, might just incorporate the discrepancies between the ideal Bondi model and the real dynamics.

Overall, we found (similarly to clusters) that the Bondi accretion models are able to satisfy our strict requirements for a plausible evolution, with a mechanical efficiency in the range 5×10^{-2}–10^{-1}. As expected, the accretion rates are always two to three orders of magnitude lower than the Eddington limit. This implies that the outflow 'touch' is always delicate and non-explosive, with power of the order of 10^{44} erg s^{-1} and velocity 10^4 km s^{-1}. These values are consistent with numerous observations of AGN outflows through absorption lines (e.g. Nesvadba et al. 2011).

In the best models, cooling rates are reduced below a few or fraction of $M_\odot$ yr^{-1}, with a monotonic decrease in time. The density radial profiles of these models do not deviate too much from the observed ones. The same can be said of the temperature gradient, with a small overheating in the inner 4-kpc nucleus. The last feature is probably associated with the continuous nature of the feedback: the Bondi formula is in fact based on the accretion of hot gas, whose reservoir never drains.

A problem for this model may be the continuous injection of energy, which carves a tunnel in the IGM. However, as shown in Section 4, this tunnel is usually very narrow and almost disappears in the surface brightness image (contrary to events associated with big bubbles). The important result is that a feeble continuous heating could operate, without being in contradiction to observations.

The creation of cavities of tens of kpc is another issue. However, we have noted that, during the increasing generation of turbulence (due to the AGN), the jet becomes gradually more disturbed: eventually, it will fragment, producing a series of small buoyant bubbles. This phenomenon is certainly enhanced by a cosmological evolution through merging and other large-scale motions (e.g. Morsony et al. 2010).

We have also checked that slightly different initial conditions, like an initial isothermal temperature profile and a NFW dark matter profile, do not alter the behaviour of the feedback, producing similar results.

5.2 Cold feedback (C)

In galaxy clusters, the triggering mechanism linked to instantaneous $\Delta M_{\rm cold}$ induces a very powerful outburst, often super-Eddington. In much less massive galaxy groups, such a powerful feedback would easily destroy the thermal structure observed, producing negative temperature gradients up to 100 kpc. Therefore, successful models adopt efficiencies about an order of magnitude lower with respect to those used for clusters. With $\epsilon_{\rm c}$ between 5×10^{-4} and 10^{-3}, cooling rates are still well below 10 per cent of the pure CF model, but now with consistent central densities and temperatures.

The model is naturally impulsive, but this time the duty cycle is very high compared to the cluster evolution shown in G11. In fact, for the majority of time, the outflow is continuous with moderate power, similar to the previous Bondi models. The AGN stays in a quiescent phase only 15–20 per cent of the time, after which it will ignite with outbursts up to 10^{45} erg s^{-1}. These powerful jets are essential for creating big bubbles of diameter 10–20 kpc.

One of such events has been analysed in Section 4 (Fig. 6). The bubble does not show high temperature within (e.g. 10^8 K or more), like in clusters (G11): it is very underdense with respect to the ambient medium, with a relatively large contrast in the SB_X map (>50 per cent). It is striking that the metal abundance is often highly asymmetric, enhanced along the outflow direction. All the previous features are commonly present in deep X-ray observations (McNamara & Nulsen 2007; Baldi et al. 2009; David et al. 2009, 2010; Gastaldello et al. 2009; Kirkpatrick et al. 2009, 2011; Rasmussen & Ponman 2009).

Overall, it is surprising that, in galaxy groups, models with cold feedback resemble, most of the time, simulations with Bondi accretion, with the merit of adding important features like X-ray cavities and ripples at larger radii (essentially weak shocks with the Mach number around 1.1–1.3). This fact clearly indicates the necessary properties of the feedback process, if outflows are the main mechanism: very frequent or almost continuous and gentle.

5.3 Bondi with cold timing (Bi)

Simulations using the third class of models, Bi, have been carried out to test the combined effect of Bondi accretion and cold triggering mode, in order to avoid Bondi continuous injection (intrinsic in the ideal case). In some preliminary tests (here not shown), we found that a simple superposition of the two feedback schemes leads to unacceptable models, because the outcome is just a more powerful jet, which carves a larger and deeper continuous channel.

Therefore, we tried another way to combine both methods. Keeping Bondi accretion prototype (entropy-regulated) for the value of power, we assumed that when the gas begins to cool at the centre (i.e. the inflow initiates), the feedback is activated. This will prevent too peaked instantaneous outflow powers and, at the same time, the AGN activity acquires a sort of duty cycle.

The results are very encouraging. The required Bondi efficiency for best models stays again in the range 5×10^{-2}–10^{-1}. Assuming $\epsilon_{\rm B} < 10^{-2}$, the evolution manifests the typical flaws of a pure CF run. On the contrary, if $\epsilon_{\rm B} > 10^{-1}$, the feedback becomes very explosive and easily 'burns' the cool core. The best Bi models show instead radial profiles with gradients not far detached from the initial observed state, along with very low cooling rates (usually one or less solar mass per year).

The look of the Bi simulations has been analysed, in depth, in Section 4. The general features are almost identical to the previous discussed models. Extensive periods of a continuous Bondi-like injection ($P_{\rm j} \sim 10^{44}$ erg s^{-1}, $v_{\rm j} \sim 10^4$ km s^{-1}) produce a narrow heating channel, alternated with dormant AGN phases (∼15 per cent). As in the cold feedback computations, the short inactivity promotes the subsequent generation of outbursts with greater power (three to four times more than the continuous phase), producing important observed features, such as tens of kpc cavities and oscillations in the flow quantities.

It is relevant to note that, as in previous good cold models, only a fraction of the injected mechanical energy is used to inflate cavities (usually under 50 per cent[9]). One of the main results, also pointed

[9] For example, the inflation energy of the bubble in Fig. 6, panel (b), is $4PV \sim 4\,(2 \times 10^{-11}$ erg cm$^{-3})\,(1.1 \times 10^{68}$ cm$^3) \approx 9 \times 10^{57}$ erg, while the

out in G11 for clusters, is that the success of a feedback crucially depends not only on the total amount of available energy, but also on how the energy is transferred to the surrounding medium. Furthermore, the heated flow has a very complex dynamics, with numerous facets. After the mechanical energy is injected into the system, a part of energy inflates the bubble, but the rest generates the cocoon and weak shocks. When the jet is more continuous, the moderate energy released at intermediate radii induces a turbulence growing in time. These chaotic motions permit a more efficient circulation of the hot gas, promoting the deposition of energy through mixing at the base of the jet, where the cooling tends to dominate. Furthermore, while the system becomes more turbulent, the feeble jet can be fragmented and can cyclically produce tiny 'bubbles', few kpc in size (albeit very faint in the SB_X map). Their buoyant motion may promote additional mixing and heating, helping the global feedback process. Quite simple feedback models still generate an amazing variety of heating processes.

As a concluding remark for these models, the efficiency comparison underlines again the strict relationship with the cold best models, exactly around $\epsilon_c \sim 5 \times 10^{-4}$–$10^{-3}$. We can therefore affirm that the feedback in galaxy groups, able to quench the CF but at the same time preserves the cool-core structure, is globally only of one type: moderate, gentle, often continuous and turbulent, with very short periods of inactivity and following outbursts.

5.4 Rejected models

It is also interesting to highlight the main features of unsuccessful models, in order to understand why some kinds of feedback do not work.

First of all, while a small part of the total energy injected could be in thermal form, above a threshold fraction of ≈50 per cent, the centre of the group becomes too hot with respect to the observations (see also Brighenti & Mathews 2002, 2003). Injection of a modest amount of thermal energy can have the beneficial effect of disrupting the otherwise ordered structure of the outflows (Section 3.5). This model intermittently eliminates the long tunnel, usually not observed in real systems. Moreover, the deposition of heat in the nucleus helps prevent the formation of a cold torus. Injection of thermal energy can be justified by assuming that shocks heat the hot IGM in the very central region.

Another rejected model considers the active outflowing mass directly linked to the real accreted mass on to the BH (InOut feedback, Section 3.6). The main problem here is that, even with very low f_{in} (e.g. $f_{out} > 0.9$), the jet velocity often exceeds $10^5\,km\,s^{-1}$. This unappealing result can in principle be fixed by adding a mass-loading factor (ηf_{out}; see also Cattaneo & Teyssier 2007; Ostriker et al. 2010). However, this assumption will mimic entrainment, just as our standard outflow generation method described in Section 2.2. It is not surprising therefore that we recover acceptable results, similar to those described in Section 5.1.

Intermittent models (Section 3.4), with fixed jet power, are only partially acceptable, as was also found for galaxy clusters (G11). The most successful run has relatively weak outflows ($P_{jet} \sim 10^{-4} P_{Edd}$, activated every 10 Myr, with a duration of 5 Myr each (model Int510m). We have also tested jets with Eddington power ($\sim 10^{47}\,erg\,s^{-1}$). As expected they will destroy the cool-core generating systems very different from the real ones.

injected mechanical energy is 2.45×10^{58} erg. Thus, the inflation energy is just 37 per cent of the total injected energy in that single event.

Probably the major flaw of the intermittent models is their artificial nature. Cooling rates can be suppressed, compared to a pure CF model, but the temperature profiles oscillate strongly at the centre. This further supports the common notion that heating *must* be self-regulated.

Finally, we have briefly investigated the effect of jet precession (not shown). Important parameters, like inclination angles and the revolution time of the jets, are currently poorly known. Nevertheless, we found that the behaviour of the cold gas at the base of the outflow, that is, the formation of a small cold torus, is not greatly different from non-precessing models. In fact, the heating channel will be again generated after the first episodes, getting a tilted orientation with respect to a normal z-axis cylindrical simulation.

5.5 Comparison with galaxy clusters

As expected, our simulations show that AGN heating has a deeper impact in galaxy groups than in clusters, because the same mechanical power per particle has a greater effect for a lighter, less bounded system.

As we have seen in the previous sections, a jet with Eddington power can easily erase the entire thermodynamic structure of the cool core. The same applies for all the self-regulated simulations with very high efficiencies ($>5 \times 10^{-3}$ for cold models; $>10^{-1}$ for Bondi). In G11, we showed that consistent cold models commonly produced super-Eddington outbursts ($>10^{47}\,erg\,s^{-1}$), with a very low frequency (∼10 per cent). Despite the huge power injected, the shock-heating phase could not destroy the observed density and temperature gradients, and the cluster quickly restored the usual cool core. The only marked consequences were more ripples at larger radii and cavities, which in the early phase presented high internal energy and shocked rims.

On the contrary, galaxy groups, with much less binding energy (per particle), cannot recover from the same strong impulsive feedback. In order to prevent such 'heating catastrophe', cold feedback models in galaxy groups require an efficiency at least 5–10 times lower. The outcome is striking, because the evolution resembles that of Bondi models, with low power jets (10^{44}–$10^{45}\,erg\,s^{-1}$) activated in a quasi-continuous gentle way. These outbursts occurring after short quiescence periods (tens of Myr) generate ∼10 kpc cavities surrounded by relatively cold rims in the region close to the centre of the group, similar to some observations (e.g. Gastaldello et al. 2009). Unlike in galaxy clusters, cavities in groups present the usual low density contrast, with temperatures similar to the surrounding medium.

The best models assuming continuous Bondi accretion, on the other hand, are equivalent in both clusters and groups (except for the efficiency, lower in groups). Accretion rates always follow a sub-Eddington regime. The moderate outflows carve a narrow tunnel in the intergalactic medium; we showed, in this paper, that it is very faint in the SB_X map and thus hard to resolve. The absence of inflated bubbles is still a riddle of this type of feedback. Note that in galaxy clusters the low-power outflows ($\epsilon_B = 0.1$) had more difficulty in halting the massive CF (tens of $M_\odot\,yr^{-1}$), showing more peaked density profiles. Therefore, in clusters, cold accretion was slightly favoured as an acceptable model.

Another common feature in both clusters and groups is the asymmetrical distribution of metals (mostly iron) produced by SNeIa in the central galaxy. They tend to accumulate along the jet axis, in qualitative agreement with recent observations (see Section 4).

In all the consistent group models, the sub-Eddington outflow powers imply that the total injected energy (a few 10^{61} erg for the

full-space system) is always an order below the total 'available' BH energy. In fact, during the simulated evolution, the BH mass increases at most 10 per cent in Bondi models. In the cold feedback model, the lower efficiencies imply a much higher $\Delta M_{\rm BH}$, similarly to galaxy clusters. As noted in G11, however, the real efficiency (still unknown) could just be higher, with a lower mass actually falling on to the BH.

Our simple approximation of the real subparsec accretion does not allow to answer why the efficiency in groups should be a factor 5–10 smaller than in clusters, besides the observational evidence that cool cores are ubiquitous and must therefore survive, to any kind of feedback (e.g. McDonald et al. 2011). It would be interesting to investigate this topic with a dedicated analysis.

6 CONCLUSIONS

Here we summarize the main conclusions of our study.

(i) Feedback triggered by both Bondi accretion and cold-mode accretion (or a combination) leads to successful self-regulated models. These schemes are able to quench the CF for many Gyr, preserving the observed thermal structure of relaxed groups. The required mechanical efficiencies for cold accretion models are in the range 5×10^{-4}–10^{-3}, while 5×10^{-2}–10^{-1} for the Bondi scenario.

(ii) In the galaxy group, the two main feedback schemes generate similar flows. The global evolution is dominated by almost continuous outflows, with the sub-Eddington power 10^{44}–10^{45} erg s^{-1} and velocities around 10^4 km s^{-1}. These values are consistent with those based on observations of AGN outflows (Crenshaw et al. 2003; Morganti et al. 2005, 2007; Nesvadba et al. 2008, 2011).

(iii) The main feature of the continuous phase is a narrow tunnel (larger than a few kpc, up to 30 kpc long), which is almost undetectable in the SB_X map. The tunnel is periodically fragmented by the increasing AGN-driven turbulence, especially when the BH is in a phase of low accretion. The products are tiny, kpc-size buoyant bubbles, which help the mixing of the IGM. These faint features are very difficult to detect, but seen in a few systems, most notably NGC 5044 (Buote et al. 2003; David et al. 2009, 2010).

(iv) Cold and hybrid accretion models show short quiescent periods (summing to a ∼15 per cent of the evolutionary time). Each quiescent period is followed by a relatively strong outburst, with power about an order of magnitude larger than the typical value during the continuous phase. The consequence is the creation of relatively large cavities (10–20 kpc), with high density contrast, in approximate pressure equilibrium with the ambient. The emission-weighted temperature in the cavity region, however, is not far above those of the surrounding medium. Feeble rims, relatively cold in the region near the centre and slightly hotter in the more distant part, with somewhat higher iron abundance, are also present. These features are again reminiscent of real systems (McNamara & Nulsen 2007 for a review; Gastaldello et al. 2009; David et al. 2009).

(v) The asymmetrical transport of metals, along the jet-axis, up to 40 kpc, is clearly visible during the active phases. In quiescent periods, the moderate turbulence promotes metal diffusion. Recent observational data confirm this behaviour (Kirkpatrick et al. 2009, 2011; David et al. 2010).

(vi) Finally, the global point of all our computations: the only possible way to heat a galaxy group, in order to suppress the grip of the CF, appears to be through a quasi-continuous 'delicate touch', while in massive clusters, rare and explosive strokes are mildly favoured over the weaker Bondi regulation. This quite different feedback evolution might explain the common observed discrepancies between the two cosmological actors. Galaxy groups are indeed not purely scaled-down versions of galaxy clusters.

ACKNOWLEDGMENTS

The software used in this work was in part developed by the DOE-supported ASCI/Alliances Centre for Thermonuclear Flashes at the University of Chicago. We acknowledge the CINECA Award N. HP10BPTM62, 2011 for making available high-performance computing resources and support. Some simulations were also performed at NASA/Ames 'Pleiades': we would like to thank Pasquale Temi as the principal support scientist at the NASA base.

REFERENCES

Allen S. W., Dunn R. J. H., Fabian A. C., Taylor G. B., Reynolds C. S., 2006, MNRAS, 372, 21
Baldi A., Forman W., Jones C., Kraft R., Nulsen P., Churazov E., David L., Giacintucci S., 2009, ApJ, 707, 1034
Blanton E. L., Sarazin C. L., McNamara B. R., Wise M. W., 2001, ApJ, 585, 227
Blanton E., Randall S. W., Douglass E. M., Sarazin C. L., Clarke T. E., McNamara B. R., 2009, ApJ, 697, L95
Böhringer H., Voges W., Fabian A. C., Edge A. C., Neumann D. M., 1993, MNRAS, 264, L25
Bondi H., 1952, MNRAS, 112, 195
Borgani S., Governato F., Wadsley J., Menci N., Tozzi P., Quinn T., Stadel J., Lake G., 2002, MNRAS, 336, 409
Brighenti F., Mathews W. G., 2000, ApJ, 535, 650
Brighenti F., Mathews W. G., 2002, ApJ, 567, 130
Brighenti F., Mathews W. G., 2003, ApJ, 587, 580
Brighenti F., Mathews W. G., 2006, ApJ, 643, 120
Brüggen M., Ruszkowski M., Hallman E., 2005, ApJ, 630, 740
Buote D. A., Lewis A. D., Brighenti F., Mathews W. G., 2003, ApJ, 594, 741
Buote D. A., Brighenti F., Mathews W. G., 2004, ApJ, 607, L91
Burns J. O., Hallman E. J., Gantner B., Motl P. M., Norman M. L., 2008, ApJ, 675, 1125
Cattaneo A., Teyssier R., 2007, MNRAS, 376, 1547
Cohn J. D., White M., 2005, Astropart. Phys., 24, 316
Colella P., Woodward P. R., 1984, J. Comput. Phys., 54, 174
Crenshaw D. M., Kraemer S. B., George I. M., 2003, ARA&A, 41, 117
David L. P., Jones C., Forman W., Daines S., 1994, ApJ, 428, 544
David L. P., Jones C., Forman W., Nulsen P., Vrtilek J., O'Sullivan E., Giacintucci S., Raychaudhury S., 2009, ApJ, 705, 624
David L. P. et al., 2011, ApJ, 728, 162
De Grandi S., Molendi S., 2002, ApJ, 567, 163D
Evrard A. E., Henry J. P., 1991, ApJ, 383, 95
Fabian A. C., 1994, ARA&A, 32, 277
Fabian A. C., Sanders J. S., Taylor G. B., Allen S. W., Crawford C. S., Johnstone R. M., Iwasawa K., 2006, MNRAS, 366, 417
Finoguenov A., Jones C., 2001, ApJ, 557, L107
Finoguenov A., Jones C., Böhringer H., Ponman T., 2002, ApJ, 578, 74
Finoguenov A., Böhringer H., Osmond J. P. F., Ponman T. J., Sanderson A. J. R., Zhang Y.-Y., Zimer M., 2005, Adv. Space Res., 36, 622F
Fryxell B. et al., 2000, ApJS, 131, 273
Gaspari M., Melioli C., Brighenti F., D'Ercole A., 2009, in Heinz S., Wilcots E., eds, AIP Conf. Ser. Vol. 1201, The Monster's Fiery Breath: Feedback in Galaxies, Groups, and Clusters. Am. Inst. Phys., New York, p. 309
Gaspari M., Melioli C., Brighenti F., D'Ercole A., 2011, MNRAS, 411, 349 (G11)
Gastaldello F., Buote D. A., Temi P., Brighenti F., Mathews W. G., Ettori S., 2009, ApJ, 693, 43
Geller M. J., Hucra J. P., 1983, ApJS, 52, 61
Giacintucci S. et al., 2011, ApJ, 732, 95
Giovannini G., 2004, Ap&SS, 293, 1

Gitti M., O'Sullivan E., Giacintucci S., David L. P., Vrtilek J., Raychaudhury S., Nulsen P. E. J., 2010, ApJ, 714, 758
Heinz S., Brüggen M., Young A., Levesque E., 2006, MNRAS, 373, 65
Jetha N. N., Hardcastle M. J., Ponman T. J., Sakelliou I., 2008, MNRAS, 391, 1052
Johnson R., Finoguenov A., Ponman T. J., Rasmussen J., Sanderson A. J. R., 2011, MNRAS, 413, 2467
Jones C., Forman W., Vikhlinin A., Markevitch M., David L., Warmflash A., Murray S., Nulsen P. E. J., 2002, ApJ, 567, L115
Kaiser N., 1986, MNRAS, 222, 323
King A. R., 2009, MNRAS, 402, 1516
Kirkpatrick C. C., Gitti M., Cavagnolo K. W., McNamara B. R., David L. P., Nulsen P. E. J., Wise M. W., 2009, ApJ, 707, L69
Kirkpatrick C. C., McNamara B. R., Cavagnolo K. W., 2011, ApJ, 731, 23
Leccardi A., Molendi S., 2008, A&A, 486, 359L
McCarthy I. G. et al., 2010, MNRAS, 406, 822
McDonald M., Veilleux S., Mushotzky R., 2011, ApJ, 731, 33
McNamara B. R., Nulsen P. E. J., 2007, ARA&A, 45, 117
Mathews W. G., Faltenbacher A., Brighenti F., Buote D. A., 2005, ApJ, 634, L137
Mellier Y., Mathez J., 1987, A&A, 175, 1
Morganti R., Tadhunter C. N., Oosterloo T., 2005, A&A, 444, L9
Morganti R., Holt J., Saripalli L., Oosterloo T., Tadhunter C. N., 2007, A&A, 476, 735
Morita U., Ishisaki Y., Yamasaki N. Y., Ota N., Kawano N., Fukazawa Y., Ohashi T., 2006, PASJ, 58, 719M
Morsony B. J., Heinz S., Brüggen M., Ruszkowski M., 2010, MNRAS, 407, 1277
Mulchaey J. S., 2000, ARA&A, 38, 289
Nesvadba N. P. H., Lehnert M. D., De Breuck C., Gilbert A. M., van Breugel W., 2008, A&A, 491, 407
Nesvadba N. P. H., De Breuck C., Lehnert M. D., Best P. N., Binette L., Proga D., 2011, A&A, 525, 43
Nulsen P. E. J., Jones C., Forman W. R., David L. P., McNamara B. R., Rafferty D. A., Bîrzan L., Wise M. W., 2007, in Boehringer H., Pratt G. W., Finoguenov A., Schuecker P., eds, ESO Astrophys. Symp., Heating Versus Cooling in Galaxies and Clusters of Galaxies. Springer, Berlin, p. 210
Omma H., Binney J., Bryan G., Slyz A., 2004, MNRAS, 348, 1105
Osmond J. P. F., Ponman T. J., 2004, MNRAS, 350, 1511
Ostriker P. O., Choi E., Ciotti L., Novak G. S., Proga D., 2010, ApJ, 722, 642
Peterson J. R., Fabian A. C., 2006, Phys. Rep., 427, 1
Peterson J. R., Paerels F. B. S., Kaastra J. S., Arnaud M., Reiprich T. H., Fabian A. C., Mushotzky R. F., Jernigan J. G., 2001, A&A, 365, L104
Peterson J. R., Kahn S. M., Paerels F. B. S., Tamura T., Bleeker J. A. M., Ferrigno C., Jernigan J. G., 2003, ApJ, 590, 207
Ponman T. J., Cannon D. B., Navarro J. F., 1999, Nat, 397, 135
Ponman T. J., Sanderson A. J. R., Finoguenov A., 2003, MNRAS, 343, 331
Puchwein E., Sijacki D., Springel V., 2008, ApJ, 687, L53
Rafferty D. A., McNamara B. R., Nulsen P. E. J., Wise M. W., 2006, ApJ, 652, 216
Rafferty D. A., McNamara B. R., Nulsen P. E. J., 2008, MNRAS, 687, 899
Rasmussen J., Ponman T. J., 2009, MNRAS, 399, 239
Ruszkowski M., Brüggen M., Begelman M. C., 2004, ApJ, 611, 158
Salomé P., Combes F., Edge A. C., 2006, A&A, 454, 437
Soker N., 2006, New Astron., 12, 38
Sternberg A., Pizzolato F., Soker N., 2007, ApJ, 656, L5
Strang G., 1968, SIAM J. Numer. Anal., 5, 506
Sun M., Vikhlinin A., Forman W., Jones C., Murray S. S., 2005, ApJ, 619, 169
Sun M., Jones C., Forman W., Vikhlinin A., Donahue M., Voit M., 2007, ApJ, 657, 197
Sun M., Voit G. M., Donahue M., Jones C., Forman W., Vikhlinin A., 2009, ApJ, 693, 1142
Sutherland R. S., Dopita M. A., 1993, ApJS, 88, 253
Tamura T., Kaastra J., Makishima K., Takahashi I., 2003, A&A, 399, 497
Tombesi F., Cappi M., Reeves J. N., Palumbo G. G. C., Yaqoob T., Braito V., Dadina M., 2010, ApJ, 521, 57
Toro E. F., 1999, Riemann Solvers and Numerical Methods for Fluid Dynamics. Springer-Verlag, Berlin
Vikhlinin A., Kravtsov A., Forman W., Jones C., Markevitch M., Murray S. S., Van Speybroeck L., 2006, ApJ, 640, 691
Voit G. M., 2005, Rev. Mod. Phys., 77, 207

This paper has been typeset from a TEX/LATEX file prepared by the author.